https://doi.org/10.5194/esd-2021-61
Preprint. Discussion started: 22 July 2021

Earth System Dynamics Discussions
Open Access
EGU

The Pacific Ocean heat engine

Roger N Jones* and James H Ricketts

Institute of Sustainable Industries and Liveable Cities, Victoria University, Melbourne, Victoria 8001, Australia

Correspondence to: Roger N. Jones (roger.jones@vu.edu.au)

Abstract

Historical warming forms a sequence of steady-state regimes punctuated by abrupt shifts. These changes are regulated by a heat engine spanning the tropical Pacific Ocean teleconnected to a broader climate network. The eastern-central Pacific maintains steady-state conditions, delivering heat to the Western Pacific warm pool. They form a heat pump with heat moving from the cold to the warm reservoir, sustained by kinetic energy. The two reservoirs exchange heat on a range of timescales, with oscillatory behaviour that intensifies under forcing. The heat engine is part of a network of oscillations and circulation interacting on a range of timescales. The process is self-regulating: steady-state regimes persist until they become unstable due to an over- or under-supply of heat for dissipation, shifting warmer or cooler to a new stable state. Pre-industrial climate was in free mode, characterised by a loosely-coupled ocean-atmosphere with limited circulation, moving into forced mode in the latter 20th century, characterised by tighter coupling and stronger circulation through the tropical Pacific with more active teleconnections globally. Continued forcing produces a stepladder-like pattern of warming. Most shifts coincide with phase changes in decadal oscillations, switching from slower to faster modes of dissipation. El Niño events combine with regime shifts to propagate heat from the oceans to land and from the tropics to higher latitudes. The most recent shift commenced in the warm pool in December 2012, ending the so-called hiatus (1997–2013), global mean surface temperatures warming abruptly by ~0.25 °C in 2014–15.

1 Introduction

The IPCC (2013) defines the climate system as a highly complex system consisting of five major components and the interactions between them. It evolves in time under the influence of its own internal dynamics and because of external forcings (IPCC, 2013).

It is unclear what this means in practice, because in everyday language complex can mean complicated, or defined formally, can represent complex system behaviour. Complicated systems can be broken down into separate parts in order to understand how those components work and reassembled as a whole. This underpins the simple to detailed modelling hierarchy first articulated in Schneider and Dickinson (1974), consistent with the constructionist hypothesis outlined by Anderson (1972).

https://doi.org/10.5194/esd-2021-61
Preprint. Discussion started: 22 July 2021


Earth System Dynamics Discussions

Complex systems on the other hand, display behaviours that include emergence, irreversibility, nonlinearity, limited predictability and self-organisation (Nicolis, 1992;Auyang, 1998;Strevens, 2009;Ladyman et al., 2013). They are not amenable to the constructionist hypothesis (Anderson, 1972). Complex systems organise at a range of scales that operate by different rules depending on scale, and may be governed by an overall organising principle. Small-world network behaviour is one example (Watts and Strogatz, 1998;Latora and Marchiori, 2001;Donges et al., 2009) and attractors in the climate system another (Nicolis and Nicolis, 1986;Dijkstra, 2019;Faranda et al., 2019).

This is the first of two papers that looks at climate through a complex systems lens, exploring how it has evolved since the pre-industrial era. It focuses on shifts in temperature, when forcing results in steady-state regimes undergoing step-like change on decadal time scales. A heat engine spanning the tropical Pacific regulates how the broader climate network responds. The second paper builds on this by presenting how aspects of this behaviour are represented in climate models, and proposes a conceptual model that represents climate as a self-organising complex system.

The paper begins by setting the context, introducing the tropical Pacific heat engine, describing how shifts in timeseries can be measured and summarises previous research, which shows that external forcing produces shifts rather than trends. It outlines the limitations of the standard approach that represents warming as gradual, describes the methods and data used, and the physical setting of the Pacific Ocean heat engine. Subsequent sections present four analyses and their results: (1) the relationship between the central Pacific, western Pacific warm pool and broader climate; (2) tracking changes in the heat engine; (3) tracking changes using teleconnections and (4) tracking causality: Granger analysis. A final section uses these results to describes the structure and behaviour of the Pacific Ocean heat engine as a heat pump and how that differs from a conventional heat engine.

2 Context and general approach

2.1 Previous research and measuring nonlinear change

In its Fifth Assessment Report, the IPCC endorsed linear warming with medium confidence, stating that "On decadal to interdecadal timescales and under continually increasing effective radiative forcing (ERF), the forced component of the GMST (global mean surface temperature) trend responds to the ERF trend relatively rapidly and almost linearly (Stocker et al., 2013)."

However, a growing body of work argues that observed climate shows regime-like behaviour. On decadal timescales, temperature follows a staircase-like pattern (Jones, 2012;Reid and Beaugrand, 2012;Jones et al., 2013;Belolipetsky et al., 2015), while over interdecadal timescales, it forms a complex trend (Jones and Ricketts, 2017). Step-like change has been reported for the atmosphere (Chikamoto et al., 2012;Jones, 2012;Belolipetsky, 2014;Belolipetsky et al., 2015;Bartsev et al., 2016;Bartsev et al., 2017;Saltykov et al.;Varotsos et al., 2019), oceans (Beaugrand, 2004;Reid and Beaugrand, 2012;Reid, 2016;Thompson et al., 2017) and in widespread ecosystem and environmental responses coinciding with these changes (Overland et al., 2008;Conversi et al., 2010;Reid et al., 2016;Beaugrand et al., 2019). These changes are usually interpreted

https://doi.org/10.5194/esd-2021-61
Preprint. Discussion started: 22 July 2021

Earth System Dynamics Discussions

as statistical artefacts of short-term random behaviour, or if accepted as genuine nonlinearities, caused by internal climate variability. Other studies have interpreted such changes as nonlinear trends (Tsonis and Swanson, 2011;Franzke, 2012;Ji et al., 2014). Collectively, these studies show largely contemporaneous shifts in the late 1970s, 1986–88 in the northern hemisphere and 1997–98 regionally and globally.

Earlier work has attributed these shifts to external forcing. For example, climate in SE Australia was stationary in the first half of the 20th century, followed by shifts in the late 1960s–early 1970s and 1997–98 that were externally forced (Jones, 2012). The 1997–98 shift is linked to regional shifts in forest fire danger and water supply (Tan and Rhodes, 2012;Jones et al., 2013).

A previous paper applied severe testing (Mayo, 1996, 2005, 2010;Mayo and Spanos, 2011;Mayo, 2018) to zonal, hemispheric and global mean temperatures (Jones and Ricketts, 2021b; referred to as JR17). The scientific hypothesis being tested was whether over decadal timescales radiative forcing produces gradual or abrupt climate responses. Six tests were developed and applied. Decadal scale regime shifts passed all six tests whereas a trend-like response failed. The updated main findings are summarised below and are outlined in more detail in the Supplementary Information (SI, Sect. S2.1).

The separation of historical temperature anomalies into shifts and internal trends leaves insufficient gradual warming to explain the minimum externally-forced warming attributed by the IPCC (2013): it is extremely likely (95–100%) that human activities caused more than half of the observed increase in global average surface temperature from 1951 to 2010 (Stocker et al., 2013, p. 60). Internal trends between change-points measure the slow component of change and the gap between one internal trend and the next measures a shift, the fast component. Fig. 1 plots GMST anomalies 1880–2018 from NCDCv4, showing total change with fast and slow components. Warming is dominated by rapid changes within periods of relative stability, with a shift to total warming ratio of 0.93.

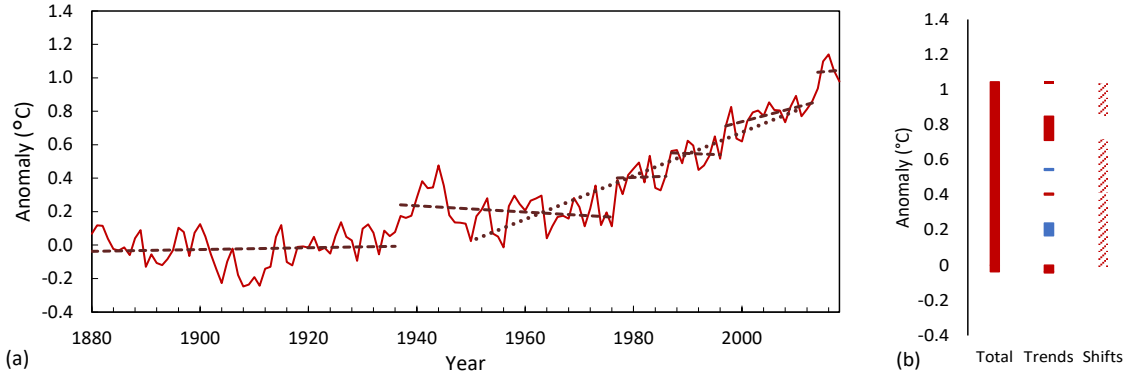

Figure 1(a) Anomalies of GMST for the NCDC record 1880–2018 showing internal trends (dashed brown lines) and the simple trend 1951–2010 (dotted line); (b) total warming, internal trends (red positive, blue negative) and shifts. Anomaly period 1880–1899.

The IPCC conclusion for warming 1951–2010 meets the criteria for severe testing because the alternatives (solar, internal variability, cosmic rays, etc) have been well tested and ruled out (IPCC, 2013). Estimating total change over that period is a

https://doi.org/10.5194/esd-2021-61
Preprint. Discussion started: 22 July 2021

Earth System Dynamics Discussions
Open Access
EGU

sampling problem, so we compare three methods: (1) shift and trend 0.63 °C, fitted linear trend 0.76 °C, 5-year average difference centred on 1951 and 2010 0.64 °C. Shifts total 0.55 °C making up between 72–86% of the total, so trend-like change cannot explain at least half that unless shifts are ignored. The average rate of change from the internal trends 1951–2010 is 0.015 °C per decade which would take at least 420 years to reproduce the minimum estimated change of 0.63 °C.

Average GMST from the CMIP5 climate model ensemble forced by historical emissions is considered by the IPCC to reproduce historical change to 2005 (Bindoff et al., 2013, FAQ10.1 Fig. 1). In JR17, GMST for 107 members of that ensemble was analysed for shifts and compared with observations. These are updated to 2018 in Fig. 2. Fig. 2a shows the pattern of shifts from regional and global average anomalies from five data sets (n=45), showing cooling shifts around 1900, small clusters around 1920, mid-1920s (coinciding with a shift in the Atlantic Multidecadal Oscillation, AMO), 1936–41, mid to late-1970s (Pacific Decadal Oscillation (PDO) shifts in 1976), 1987–88 (northern hemisphere, NH), 1997–98 (PDO shifts in 1998), 2013–14 (PDO shifts in 2014).

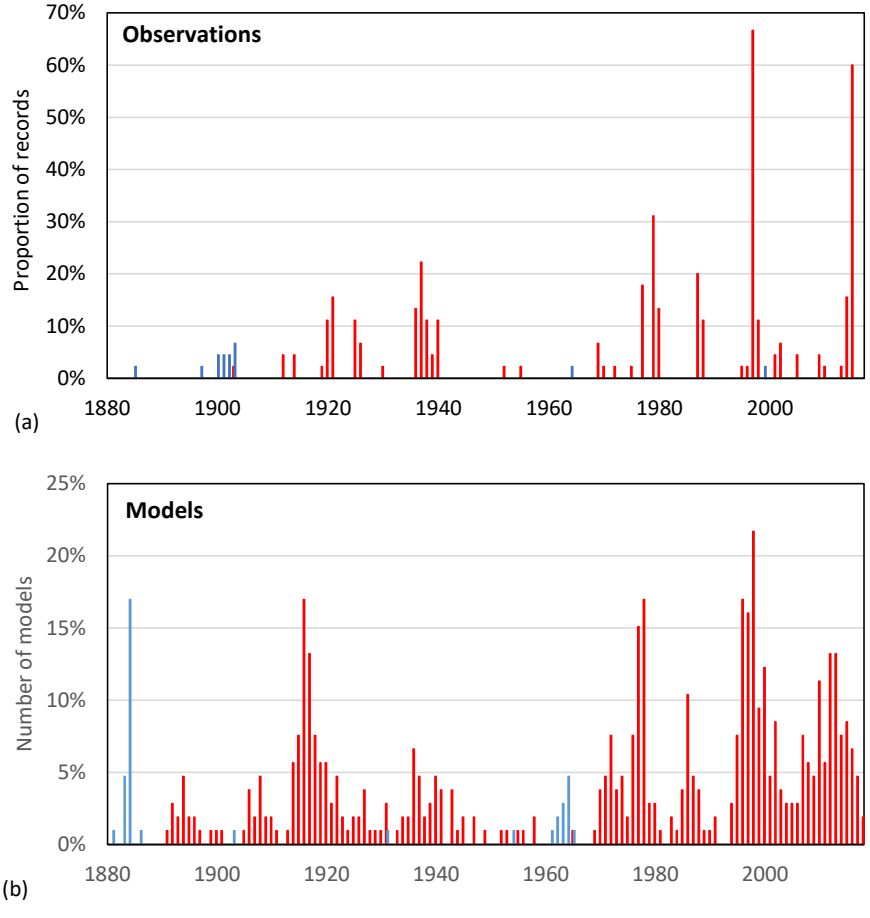

Figure 2(a) Shift dates for 45 records of mean anomalies from zonal, hemispheric and global regions for up to five records, updated to 2018; (b) Shift dates for a 107-member ensemble from CMIP5 RCP4.5 mean GMST anomalies 1880–2018 (historical emissions to 2005).

https://doi.org/10.5194/esd-2021-61
Preprint. Discussion started: 22 July 2021


Earth System Dynamics Discussions

The climate model ensemble (n=107) reproduces the observed pattern from the 1936 peak in Fig. 2a, earlier showing a peak around 1916 and negative shifts associated with the simulated Krakatoa eruption in 1883 and the later Agung eruption in 1963 (Fig. 2b). The correlation between the models and observations to 2005 is 0.33 ($p<0.001$). Shifts following volcanic forcing in Fig. 2b shows the influence of both positive and negative forcing on the timing and direction of shifts (Reid et al., 2016;Jones and Ricketts, 2021b).

Total shifts in the model ensemble 2006–2095 correlate with equilibrium climate sensitivity (ECS, 0.73 n=94), total steps 0.82 and internal trends 0.43, all $p<<0.01$. However, correlations between ECS and total shifts, total trends and warming during the historical period 1861–2005 are low, being 0.04, -0.12 and -0.03 respectively (n=94). During the historical period, intervals with strong negative volcanic forcing counteract those with positive radiative forcing. for total shifts, trends and warming are 0.73, 0.43 and 0.82. For 2006–2095, steps, shifts and internal trends expressed as r^2 values are 0.53, 0.18 and 0.66, respectively, giving shifts 2.9 times the influence on ECS compared to internal trends. This is consistent with abrupt heat releases from the shallow ocean causing rapid atmospheric feedback. It is not consistent with radiative forcing causing a gradual response in surface temperatures.

In JR17, we concluded that the shallow ocean–atmosphere system contains a heat storage and release mechanism. Radiative forcing has a nonlinear response on decadal timescales which follows a complex trend over longer time periods. These are consistent with the separation of the climate system into linear radiative and nonlinear dissipative components by Ozawa et al. (2003). This prompted a search for the mechanisms and processes regulating the storage and release of heat over decadal timescales.

2.2 A heat engine in the Pacific Ocean

Analysing the 2003–15 satellite sea level record, Peyser et al. (2016) identified a large outburst of water from the Western Pacific Warm Pool to the east, temporarily altering sea level by up to 200 mm. This large expenditure of kinetic energy coincided with the 1997–98 shift in temperature, suggesting it could be part of a storage and release mechanism. A similar event in 2014–15 (Yin et al., 2018), coincided with the next shift.

Peyser et al. (2016) identified two regions from first Empirical Orthogonal Function (EOF) analysis of AVISO satellite sea level data 2003–15 that describe two ends of a sea-level see-saw: the western Pacific (120° E–180° E and 20° S–20° N), situated over the centre of the Western Pacific Warm Pool, and the eastern (central) Pacific (100° W–160° W and 20° S–20° N), almost fully superimposed over the Niño 3.4 area (Fig. 3). The sea level satellite record is too short to reveal multidecadal patterns, so we analysed sea surface temperatures from ERSSTv5 for shifts: namely temperature of the warm pool, TWP, and of the east central Pacific, TEP.

The results are shown in Figure 4. TWP shows step changes in 1902 of -0.34±0.007 °C, 1921 0.17±0.007 °C, 1942 0.21±0.006 °C, 1978±0.006 0.17 °C, 1995 0.28±0.008 °C and 2013 0.28±0.041 °C (Fig. 4a). TEP is very different, with no change until a shift in 1997 of 0.47±0.006 °C (Fig. 4b), with potentially a second in 2014 at p=~0.13 (changing the two into 0.45±0.007 °C and 0.47±0.023 °C, averaging 0.46 °C). An average of 0.46 °C will be used for TEP from this point forward.

https://doi.org/10.5194/esd-2021-61
Preprint. Discussion started: 22 July 2021

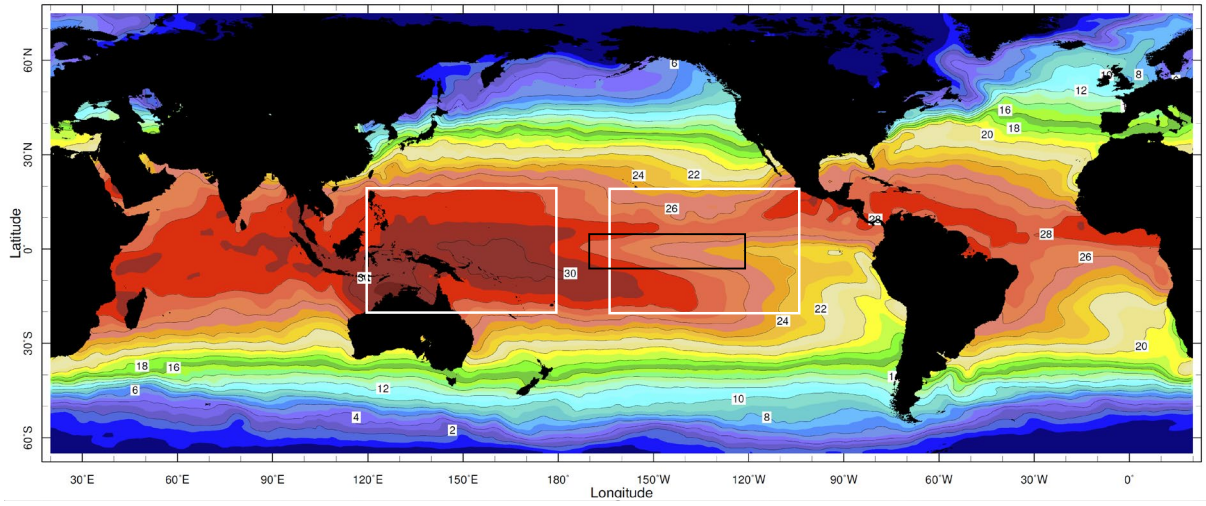

Figure 3 Mean sea surface temperatures from Dec 2012 showing the TWP, TEP and Niño 3.4 areas.

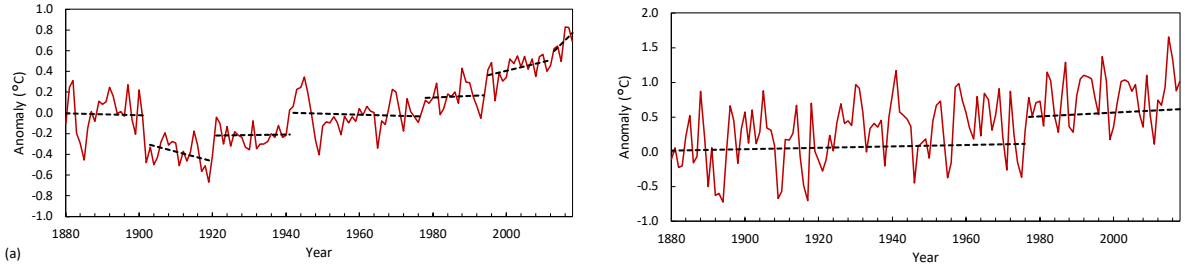

Figure 4 Anomalies of TWP (a) and TWEP (b) for the NCDC record 1880–2018 showing shifts (red) and internal trends (dotted lines).

Following the negative shift in 1902, TWP closely follows GMST. For the five records analysed in JR17 (BEST, Cowtan and Way, GISS, HadCRU and NCDC), two shift in 1920, one in 1930, four in 1937, one in 1977, two in 1979, two in 1980, one in 1987, five in 1997, one in 2013 and four in 2014. The NCDC record in Fig. 1 registers upwards shifts in 1937 of 0.22±0.003 °C, 1977 0.19±0.005 °C, 1987 0.14±0.011 °C, 1997 0.23±0.005 °C and 2014 0.27±0.010 °C. The two positive shifts in TEP coincide with changes in PDO phase, whereas earlier PDO phase changes remained stable.

The largest difference is between the TWP shift in 1942, and the shifts in 1937 GMST and various SST records. Adjustments made to pre-WWII and WWII data in ERSSTv4 and v5 have moved this date later than in earlier versions (SI, Sec. S1.5). WWII SST data is biased warm in some regions (Liu et al., 2015), affecting the southern tropics and southern hemisphere and warm pool, a region of conflict at the time. This produces a scatter of shifts 1936–40 in Fig. 2, whereas in the equivalent chart in JR17 from ERSSTv3, shifts clustered around 1936–37.

The correspondence between TWP and GMST led us to consider that the warm pool may act as a thermostat and that the relationship between TEP and TWP, the convective role of TWP and the involvement of the two in the ENSO cycle, suggested the presence of a heat engine.

https://doi.org/10.5194/esd-2021-61
Preprint. Discussion started: 22 July 2021


Earth System Dynamics Discussions

155 **2.3 Approach and methods**

The relationship between shifts in TWP, TEP and broader climate is explored in Sect. 3.1. Shifts are detected using the multi-step bivariate test as in JR17 (Jones and Ricketts, 2017;Ricketts and Jones, 2018;Ricketts, 2019). Details of data sets, test and full results for the shifts are listed in the SI, in addition to extensive post-processing testing for false positives. Analyses include tracing shift timing and location. Temperatures from NCDCv4 (incorporating ERSSTv4) and ERSSTv5 are
160 the main data sets investigated (see full methods and data in SI). The NCDCv4 temperatures include the 30° zonal averages from all regions except 60 °S–90 °S, the central tropics 20 °N–20 °S, both hemispheres and GMST from land-ocean, land and ocean. TWP and TEP are sourced from ERSTTv5 because its higher resolution is an advantage in the Indonesian archipelago. This provides a total of 29 regions for analysis. The timing of shifts between the heat engine and other regions is used to identify a flow network for the dissipation of heat. An additional analysis of SST from the Pacific and Atlantic
165 basins from ERSST v5 is used to track shifts in more detail.

Shifts in lag-1 autocorrelation are also assessed for major variables (GMST, global land, global ocean, TWP and TEP), are analysed using Rodionov's (2015) regime shift test (Section 3.1.2). A simple tracking model for TWP has been developed to test the thermostat hypothesis. A rolling 6-month average of temperature above threshold is calculated to see where the build-up of heat precedes a regime shift (Section 3.2). If TWP is acting as a thermostat, shifts in the heat engine would
170 precede those elsewhere. The relationship between temperature and PDO, AMO and the Atlantic Meridional Overturning Current Index (AMOC) indices is explored to see whether the broader teleconnected system is behaving like a network with respect to the temperature shifts (Section 3.3).

A Granger-type regression analysis, suggested by a reviewer, is used to perform two-way lagged regression analysis between pairs of time series across the different regions, comparing their stationary and non-stationary relationships. Testing was
175 carried out using the Real Statistics resource pack (Zaiontz, 2018). It requires stationary time series, needing steps or trends to be subtracted from non-stationary timeseries. We test the de-stepped stationary and the raw nonstationary time series. The stationary time series shows relationship during regime periods and comparing those with the results from raw data shows the influence on and impacts of regime shifts. The nonstationarity invalidates p-values, but the f-test results convey valuable information when compared with the stationary results.

180 Stationary and raw timeseries of all 29 records on annual and monthly timescales are separated into the periods 1880–1967 and 1968–2018 for the analysis. Tests carry though to lag-24 where possible, and lag-15 for annual data from 1968. The outputs produce 29 x 29 matrices and show the lagged influences of temperature between ocean-land, ocean and land, on a zonal, hemispheric and global basis plus TWP and TEP. Each matrix is transposed to assess heat moving from and to each region. Limited tests involving the PDO and AMO indices are also carried out.

185 Correlation matrices for the same data are also produced, and selected lagged correlations calculated to test the direction of influence. Correlation at time t=0 reflects direct influences such as those due to circulation (monthly, annual) and direct teleconnections (annual). Correlation does not show the direction of flow but the Granger causality data at time t=1,2, … n

https://doi.org/10.5194/esd-2021-61
Preprint. Discussion started: 22 July 2021


Earth System Dynamics Discussions

can show the likely direction at time t=0, indicated by the direction of short-term lags and through lagged correlation. These can be one-way or two-way. A full description of each test and the data used is in the SI.

To avoid assumptions about the nature of what constitutes forced and unforced behaviour, we do as little pre-processing as possible. This approach exceeds the design limits of some tests and those instances are flagged. Where stationary time series are required, we remove steps rather than detrending.

2.4 Pacific Ocean heat engine physical setting

The main roles of the tropical Pacific Ocean warm pool in a changing climate are understood as (Clement and Cane, 1999;Pierrehumbert, 2000;Gagan et al., 2004;De Deckker, 2016):

(i) its role as a source of large-scale convection, distributing latent heat and providing uplift feeding into meridional heat distribution (i.e., away from the equator),

(ii) its role in ENSO, distributing heat in El Niño and cooling in La Niña events,

(iii) exhibiting decadal variability through the PDO and linked mechanisms including its modulation of the ENSO cycle, and

(iv) warming and expanding under global warming (Cravatte et al., 2009;Weller et al., 2016), while also being modulated by decadal variability.

As the largest single source of heat from the tropical regions the western Pacific or Indo-Pacific Warm Pool has been called global climate's heat engine (Quinn et al., 2006;Cravatte et al., 2009;Ma and Yu, 2014;De Deckker, 2016), or the firebox for the global heat engine (Simpson, 1988). It covers the area of the western Pacific and eastern Indian Ocean with sea surface temperatures (SSTs) above 28.0 °C or 28.5 °C. A region of enormous evaporation and convection, the warm pool transports latent heat into the atmosphere, fuelling the East Asian monsoon and linking to other monsoonal systems (Pierrehumbert, 2000). The resulting rainfall feeds a body of fresher, warmer and less dense seawater that sits on a thermocline up to 80 m deep (Bosc et al., 2009).

The cold tongue comprised of upwelling cooler waters in the eastern and central Pacific, acts as the collection area for the heat engine. Winds and currents move heat being absorbed into the shallow ocean across over 15,000 km of the tropical Pacific east to west (Fig. 5). This is 'uphill' in terms of temperature and sea level, with a 6–8 °C difference from the far east to the west and 400–500 mm in sea level (Wyrtki, 1975a;Harries et al., 1983;Bigg, 1990). This process is bolstered by strong internal feedbacks (Dijkstra and Neelin, 1995) keeping SST in the central Pacific relatively constant. The thermocline, a dense boundary separating shallow, lighter warm water from deeper, denser cool water forms a wedge, shallow in the east and deeper in the west. The eastern edge of the warm pool is separated from the cooler Pacific by a sharp salinity front (Bosc et al., 2009;Cravatte et al., 2009), the location of which is important for ENSO dynamics (Picaut et al., 1996;Maes et al., 2006). In normal, steady-state conditions the westward movement of wind, water and warmth keeps the system stable. The

https://doi.org/10.5194/esd-2021-61
Preprint. Discussion started: 22 July 2021

Earth System Dynamics Discussions
Open Access
EGU

surface winds that blow east to west return at altitude and subside, forming the Walker Circulation (Fig. 5)(Bjerknes, 1969;Julian and Chervin, 1978;Gill, 1980).

Fig. 5 shows a simplified subsurface return flow in plan but in reality, there are several (Hu et al., 2020). This includes the north and south Pacific countercurrents (Wyrtki, 1973;Wyrtki, 1975b) and a subsurface return current about which little is known (Li et al., 2020). East-west exchange also varies on a seasonal basis and with ENSO events. Meridional return flows have a longer circulation time. Hu et al. (2020) provide an extensive review of the warm pool and its links.

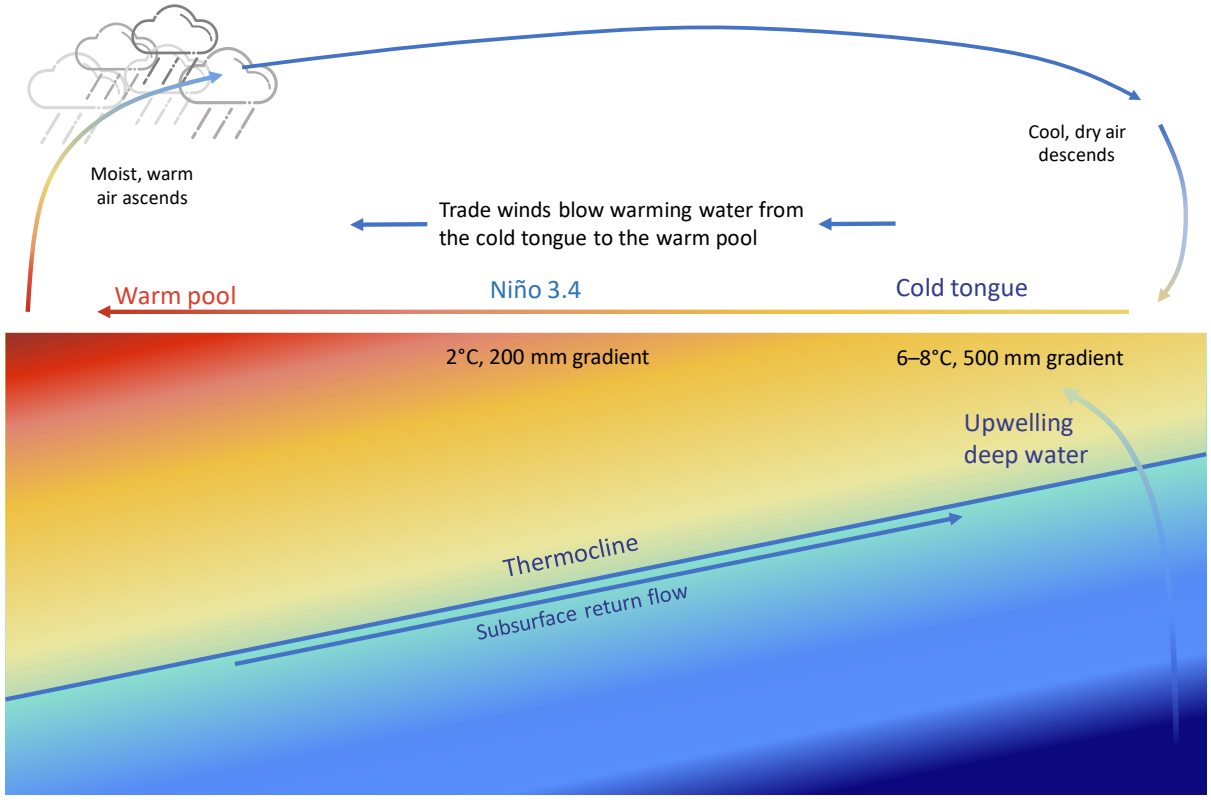

Figure 5 Cross section of heat engine showing the Walker circulation, warm pool and cold tongue.

During an El Niño event, winds turn east and the thermocline tilts the same way, heating the eastern Pacific and the atmosphere. During a La Niña event, upwelling cool waters are blown west as the thermocline shallows in the east and conditions are generally cooler. This heat engine is the reverse of the classical Carnot heat engine where heat moves from the hot to cold reservoir (Kleidon, 2016). A corollary of the second law of thermodynamics states that energy can only flow from cold to hot components of a system unless external work is being done (Kleidon, 2016). This distinguishes the heat engines in the tropical Pacific and Atlantic from most others.

The external work is provided by incoming radiation being converted into kinetic energy, directed by trade winds produced by the Coriolis effect and by internal positive feedback effects (Sverdrup, 1947;Neelin and Dijkstra, 1995). Interannual to decadal and possibly longer oscillations are part of the Pacific heat engine, influencing its behaviour. These states reflect the

https://doi.org/10.5194/esd-2021-61
Preprint. Discussion started: 22 July 2021

Earth System Dynamics Discussions

basic structure of ENSO, which responds to forcing on timescales from interannual to millennia (Cane and Clement, 1999;Clement and Cane, 1999;Pierrehumbert, 2000).

Even if global climate considered to be in equilibrium with incoming solar radiation, internally, it is always in a state of disequilibrium (Leith, 1975;Trenberth and Hurrell, 1994;Kleidon, 2009, 2012). In order to return heat into space at the radiative height of the atmosphere, the tropics have an excess of energy gained and the high latitudes a deficit, so heat moves from the equator to the poles on a continual basis. Various mechanisms within the climate system are involved in dissipating this energy, which is mediated by meridional heat transport (Bryan, 1962;Wunsch, 2005). These mechanisms can be stable, periodic or non-periodic. Two major stable heat engines on each side of the central Pacific are the north and south Hadley Cells. These lift moist, tropical air that rains out and descends in the mid latitudes as dry air (Pierrehumbert, 2000). Subsurface heat is also transported away from the tropics in stable ocean eddies.

Internally generated climate variability is largely a product of oscillations that couple the shallow ocean and atmosphere, such as the El Niño-Southern Oscillation (ENSO) and Pacific Decadal Oscillation (PDO; Mantua and Hare, 2002), producing climate regimes. These regimes switch between different modes, maximising the potential to transport heat from warm to cold regions in the most efficient manner. Efficiency here is a loaded concept because energy in climate can be transported through radiation, conduction and convection, each requiring different levels of 'work' (Kleidon 2016; including radiative exchange that does no kinetic work (Delgado-Bonal, 2017)). Distinguishing free from forced behaviour is therefore very difficult (Lorenz, 1979;Kleidon, 2016).

3 Results

3.1 Relationship between TEP, TWP and broader climate

This section presents a more detailed assessment of TEP, TEP, GMST and regional temperature change. Figure 6a shows anomalies from pre-industrial temperature (1880–1899) for TEP, TWP and GMST, highlighting the similarity between TWP and GMST after 1902. Figure 6b shows the difference between TEP and TWP, which maintains an average of 1.94 °C over time. Mean TWP is 28.20±0.31 °C and TEP 26.26±0.44 °C. The overall east-west gradient across the Pacific is a critical influence on ENSO behaviour (Kim and An, 2011).

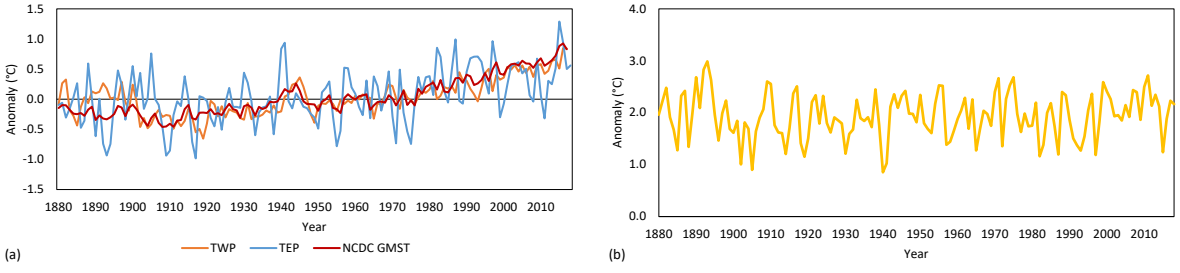

Figure 6(a) TWP, TEP and GMST (NCDC) anomalies (1880–2018, 1880–1899 baseline); (b) TWP-TEP temperature gradient over the same period.

https://doi.org/10.5194/esd-2021-61
Preprint. Discussion started: 22 July 2021


Earth System Dynamics Discussions Open Access EGU

Warming from 1880–1899 is 1.05 °C for GMST, 0.77 °C for TWP and 0.62 °C for TEP. The lower totals for TWP and TEP are because warmer temperatures in the late 19th century were followed by abrupt cooling in TWP in 1902. TWP closely tracks GMST from the post-1902 low. The correspondence between Pacific temperature and GSMT has been noted previously (Cane, 1998;Pierrehumbert, 2000), Pierrehumbert (2000) commenting on the inherent tippiness of the tropical Pacific.

Annual analyses were carried out for all 29 temperature records, the PDO and AMO indices, backed up by monthly analyses to pinpoint the specific timing for each shift. The monthly analyses do not use any pre-set p values, but rely on a matching annual shift of $p<0.01$, which some cases, is relaxed to $p<0.05$. The overall pattern for the timing of shifts is similar to that in Fig. 2a. A full record is detailed in Table S8. An additional set of analyses for the Pacific and Atlantic Ocean basins to help pinpoint the origins of shifts are presented in Table S9.

3.1.1 Early 20th century shifts

Shift dates during the early 20th century may be less reliable because of issues with data quality and coverage, especially those in the tropics before and during WWII as raised earlier. Early shifts include NH land in mid-1893 and the PDO shifts positive in July 1896, the latter associated with drying on several continents (Whetton et al., 1990). The next series of shifts span 1901–03, nearly all associated with SST. The AMO shifts negative in Apr 1902 followed by TWP in May 1902 but the earliest shift detected is in the Atlantic 40–60° N and Pacific 30–60° S in May 1900, followed by 30–60° N Atlantic, Pacific and global and southern hemisphere (SH) and NH oceans. Other regions follow in 1902 and 1903, mostly ocean-based. The SH ocean and land-ocean shifts cooler in mid-1901 and 30–60°N in Nov 1901. The AMO index shifts negative in April 1902 and downward shift in TWP followed in May. Positive shifts in late 1911 in SH ocean and in late 1914 in the NH ocean may be a partial recovery.

The next series occur in 1919–21. The high northern latitudes shift positive in mid-1919, TWP responds in Nov 1920, global land in Dec 1920 and NH land in Jan 1921. This only positive shift in TWP not associated with an El Niño, occurring just before a strong La Niña event in 1921 (Wolter and Timlin, 2011). A series of shifts from 1924–25 occur mainly in the tropics and NH, culminating in positive regime shifts in the PDO in Sep 1925 and AMO in Dec 1925. The bivariate test run on 5° x 5° gridded data shows shifts forming the horseshoe pattern of the AMO signature in the northern Atlantic (Ricketts, 2019).

The NH shifts 1920–25 may have been partially driven by increasing incident solar radiation, which set an early peak around 1920 (Egorova et al., 2018;Hegerl et al., 2018;Wang et al., 2018). Analysing the different forcings of the early 20th century, Meehl et al. (2003) suggest that much of the warming (from the 1920s to 1940s) was due to solar forcing, especially in areas experiencing radiation increases. The land-ocean warming ratio was 2.6–2.7 compared to 1.3–1.5 later in the century. This supports the idea that the Pacific Ocean was responding to NH-dominated warming.

The 1937 shift is first recorded in tropical and SH oceans but can be detected in global SST. Australian mean annual SST shifts upwards (1938) with land temperatures unaffected. The Indian subcontinent and low-latitude South America may also

https://doi.org/10.5194/esd-2021-61
Preprint. Discussion started: 22 July 2021


Earth System Dynamics Discussions

have shifted upwards, based on the analysis of 45° longitude, 30° latitude zonal segments (not shown). Data issues in the tropics and SH just before and during WWII make it difficult to pinpoint exact times and locations.

This period is followed by what Broecker (2005) called the long pause. No shifts are detected until April 1957 for NH tropical and SH land. This coincides with shifts in minimum temperature in parts of Australia, a sign of adjacent increases in SST. Powell Jr and Xu (2015) detect regime changes in surface wind stress 1956–57 across all three major ocean basins.

The 1902 shift of -0.34 °C in TWP took until 1937 to recover fully, suggesting a scenario where oceans cooled at the turn of the 20th century and positive forcing, mostly over land, led to a subsequent recovery. Warming to 1880–1968 is 0.10 °C for global SST and 0.47 °C for global land, larger than the land-ocean warming ratios noted by Meehl et al. (2003).

Shifts identified in the second part of the record are described in detail in Section 3.2. They are 1968–69 initiated in TWP, affecting the SH; 1976–78 initiated in TEP and propagating globally; 1986–88 initiated in the NH tropics and affecting the NH, 1995–98 where a regime shift in the AMO index is immediately followed by TWP and propagating globally, 2008–09 SH in the Australian region, 2012–15 initiated in TWP and propagating globally.

3.1.2 Shifts in autocorrelation

Beaulieu and Killick (2018) detected a change in autocorrelation in historical GMST, analysing five records and identifying a breakpoint in either 1962 or 1972, with high autocorrelation before the change point and low (whitened) afterwards. To see whether these changes are regime-like, the NCDC data was de-stepped and analysed for shifts in lag-1 autocorrelation using Rodionov's (2015) test. GMST contains an abrupt shift in autocorrelation, from 0.59 in 1881–1968 to 0.01 in 1969–2018 (p=0.0001; Fig. 7b). This implies an abrupt and widespread change in behaviour. The cumulative sum of lag-1 residuals for GMST indicates the presence of random walks in the first part of the series, whereas the second part is relatively flat denoting white noise (Fig. 7a).

Autocorrelation in SST shifts from positive to neutral in 1914 and back to positive in 1938 (0.74 to 0.09 to 0.74, p=0.002, 0.01), shifting neutral again in 1957 (0.74 to 0.22, p=0.01; Figure 7c). Land temperature autocorrelation shifts in 1972 from 0.35 to white (-0.07, p=0.02; Figure 7d). TWP follows a similar pattern to SST, shifting from positive to negative in 1923 and back to positive in 1941 (0.32 to -0.31 to 0.62, p=0.03, 0.001), and shifting neutral again in 1972 (0.62 to 0.05, p=0.005; Figure 7e). TEP remains constant at 0.28, so is not shown. The timing of shifts in SST and TWP coincides with warming periods in both variables, with autocorrelation being higher during periods of little or no warming. Land temperature is less responsive, not whitening until 1972.

Regions do not reflect these large-scale patterns. Regional variations show whitening later in the record for the ocean south of 30° N, whereas the higher latitude oceans become more autocorrelated. Zonal temperatures over NH land whiten in the early 20th century, responding to regional forcing and the dissipation of heat polewards. SH land autocorrelation becomes negative after 2000 (-0.40, p<0.01) showing the increased influence of ENSO (Details in Sect. S3.3).

Figure 7(a) Cumulative sum of residuals of NCDC GMST 1881–2018 after removal of steps showing annual data and 11-year running means; (b) shifts in correlation between lag-1 difference GMST with steps removed (Rodionov (2015) with target p<0.05, cutoff length = 20, tuning constant = 3σ); (c) as for (b) but ocean only; (d) as for (b) but land only; (e) as for (b) but TWP.

https://doi.org/10.5194/esd-2021-61
Preprint. Discussion started: 22 July 2021

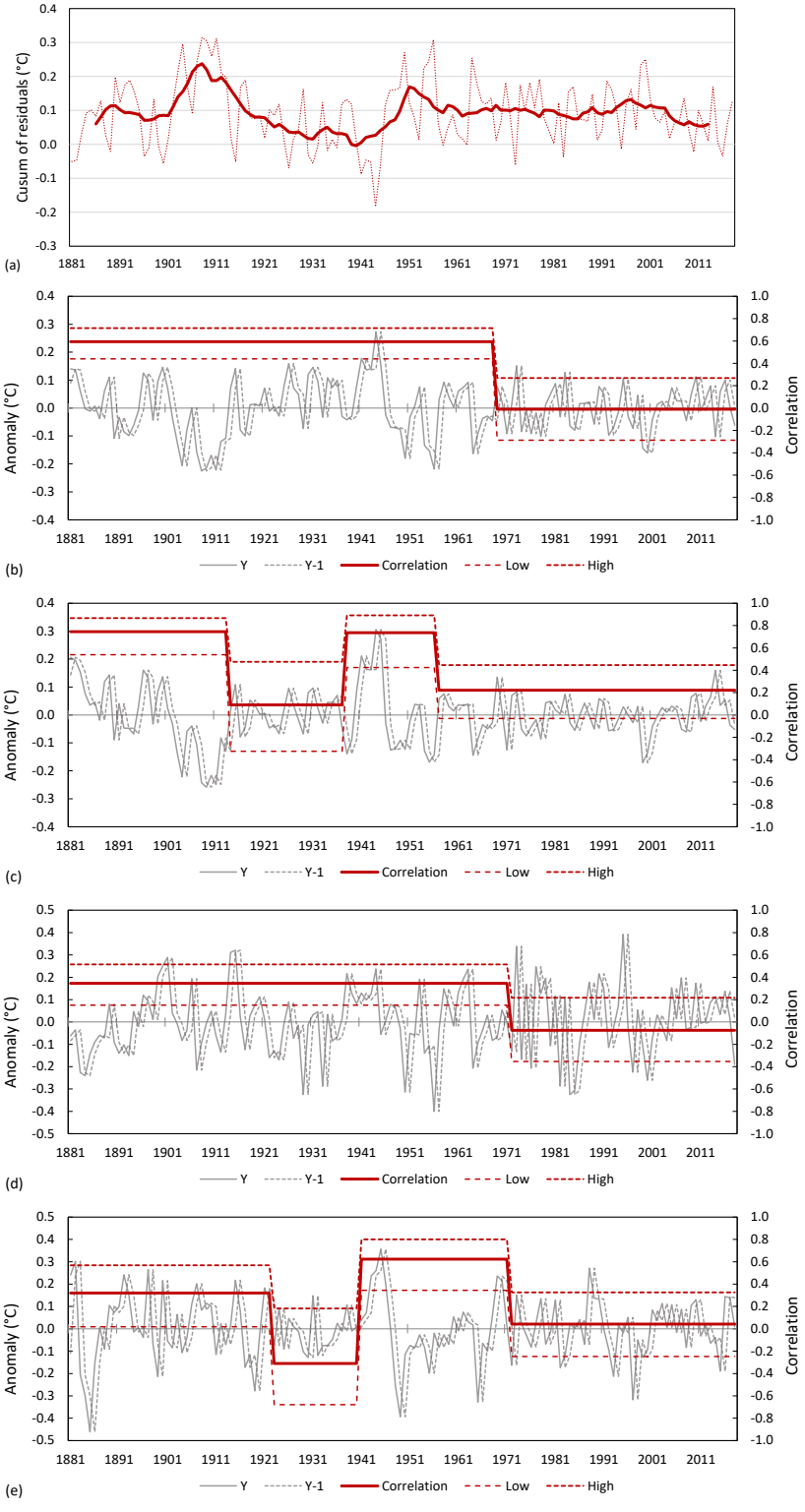

330

https://doi.org/10.5194/esd-2021-61
Preprint. Discussion started: 22 July 2021


Earth System Dynamics Discussions

335 Based on these and other results described in the paper, we have separated historical climate into free and forced modes. Based on the timing of the positive shift in TWP in 1968 encountered during the tracking exercise and global shift in 1969, 1880–1967 is selected as free mode and 1968–2018 as forced mode. The staggered whitening dates between ocean, land and ocean-land indicate no single change point but a succession of events completing the transition. The analyses for free and forced modes presented in the rest of the paper are insensitive to the exact date of change.

340 Free mode denotes a more relaxed state where temperature is free to move away from its current regime average influenced by decadal climate variability. This mode may also act as a neutral climate state, which can warm under positive forcing and can cool under negative forcing. In forced mode, the whitening of temperature data is consistent with the heat engine doing more work in dissipating energy. The statistical representation of this mode is a steady-state mean surrounded by normally-distributed noise.

345 **3.2 Tracking changes in the heat engine**

From the 1960s (possibly from 1957), the tropics led warming shifts. This is consistent with a build-up of excess heat in the tropics and ensuing instability, requiring a succession of regime shifts to warmer states. A tracking model follows the build-up of heat in TWP and shifts in TWP. The model uses monthly data, beginning in Jan 1947 to avoid the poorer data quality of the WWII period (See Folland et al., 2018). Initialised with the estimated mean (1946 is an inhomogeneity), each month

350 the cumulative and six-month running means are calculated, along with the difference between the two. If a difference of >0.2 °C is sustained for a period of up to 48 months, a shift is considered to have occurred. A similar exercise could not be undertaken for TEP because of its dynamic nature (seven times the variance of TWP), continually losing heat to TWP and through ENSO events. The propagation of shifts through the global climate network was tracked for each event. Further information is in the SI Section S2.1 with more detailed results in Section S4 and detailed timing in Tables S8 and S9.

355 Fig. 8a shows successive regimes for monthly TWP and TEP 1960–2018. A regime shift takes some time to register statistically at $p<0.05$ or $p<0.01$ – from two to fifteen years depending on the size of the shift and the background variance. A pre-detection period of 48 months is shown as a dotted line. For TWP, four shifts are nominated, including 1968 at $p<0.05$. Two shifts for TEP are shown, 1976 and 2014. The latter had not reached the $p=0.05$ threshold by 2018, but exceeds one standard deviation, which would achieve that if sustained. Only one period previously has exceeded this threshold

360 without undergoing a shift: a four-year sequence in 1960, taking in 1957–58 (there is an exceedance during the 1940s but data quality is compromised). Checking with ERSSTv4 and v5 data to 2020, the shift remains in place with p values unchanged, but with only six years post-shift, its magnitude remains uncertain.

Fig. 8b shows the six-month TWP anomalies that exceed 0.2 °C. Two events not associated with regime changes shown in Fig. 9a are labelled: the 1987–88 shift in the NH and 2010 shift in the SH. The only outlier not directly associated with

365 widespread regime change was in 2001, this date shows up in a few annual shifts in the tropics and high northern latitudes, most of which do not carry through to monthly data (Table S8).

https://doi.org/10.5194/esd-2021-61
Preprint. Discussion started: 22 July 2021

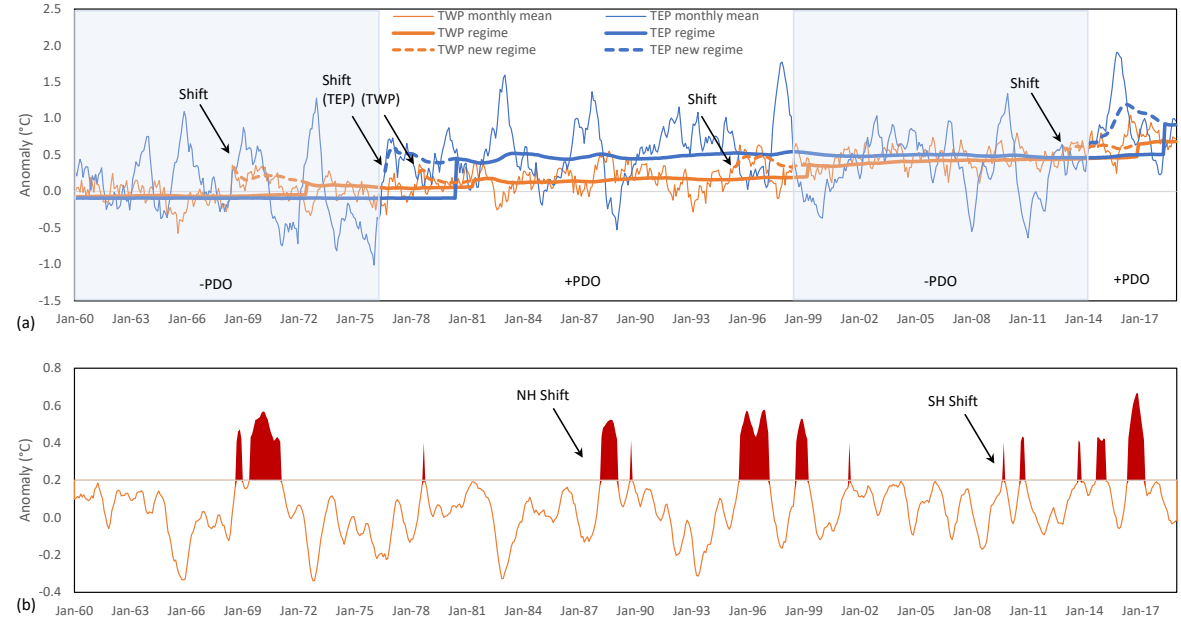

Figure 8 Tracking model for the heat engine showing (a) monthly anomalies for TWP and TEP from ERSSTv5 and cumulative means for current regime (pre-detection dashed) noting the timing of the shifts detected for four regime changes in since 1947 along with PDO phases (light blue shading), (b) six-month retrospective mean showing 0.2 °C exceedances from the cumulative mean (red shading) and the two shifts not associated with shifts in TWP.

Six events can be identified: 1968–69 (SH, Fig. 9), 1976–79 (global, Fig. 10), 1986–88 (NH, Fig. 11), 1995–98 (global, Fig. 12), late 2000s (mainly SH), 2013–15 (global, Fig. 13). All are documented except the late 2000s event. Fig. 8 shows the shift in TWP occurs May 1968 followed by 60° S–30° S ocean and land-ocean in Dec 68, with a sustained anomaly in TWP to Sep 1971. These shifts affected Australian SST and land temperatures in southern Australia, coinciding with a downward shift in winter rainfall in SW western Australia (Jones and Ricketts, 2019). The following El Niño event in 1972–73 is linked to an increase in northern Australian rainfall of 19% and warming along the east coast of Australia (Jones and Ricketts, 2019).

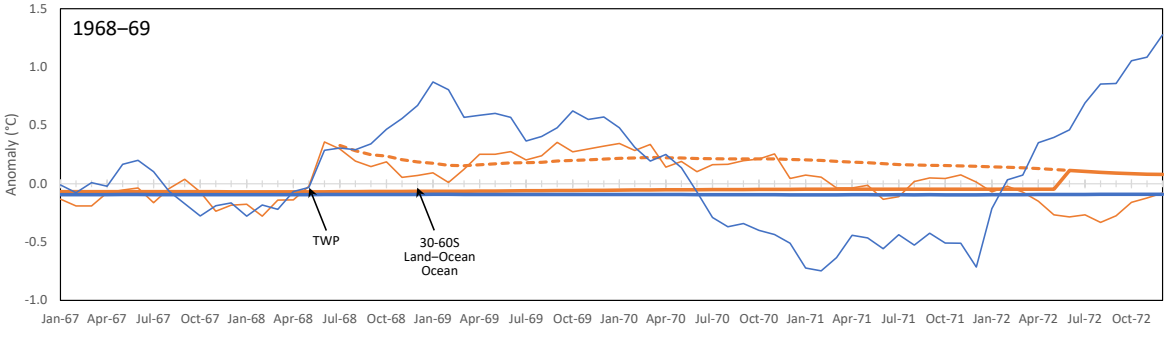

Figure 9 Sequence of shifts 1967–1972, key shown in Figure 8a. Shift timing in Table S8.

https://doi.org/10.5194/esd-2021-61
Preprint. Discussion started: 22 July 2021

Earth System Dynamics Discussions
Open Access
EGU

The 1976–78 event commences with a positive shift in the PDO in Jul 1976 and TEP in Aug 1976 (Fig. 10). The sequence shows ocean then land-based warming in the SH in 1976–77, followed by NH warming in 1978–79. The SH shifts are prompted by the TEP. TWP responds in May 1978, followed by more general warming in the NH tropics, finally registering as a global phenomenon in mid-1979.

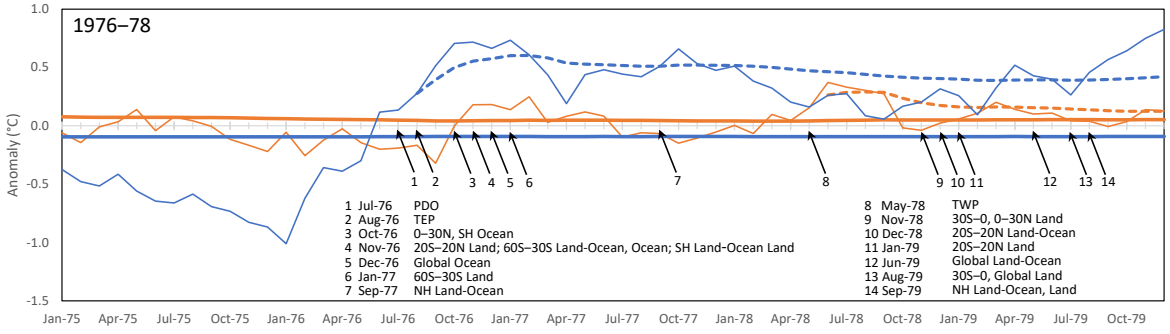

Figure 10 Sequence of shifts 1975–1979, key shown in Figure 8a. Shift timing in Table S8.

The origin of the 1986–88 event is difficult to locate, showing up first in the tropical ocean 0–30° N in Oct 1986 ($p<0.10$ annually) and in the global oceans in Dec 1986 before propagating through the NH during 1987–88 (Fig. 11). This may be due to a large-scale change in circulation. After the initial ocean shift, the regime shift appears to be largely in the atmosphere and over land, its main impacts felt in western Europe and parts of North America, coinciding with the 1988 drought. Its impacts are comprehensively documented by Reid et al. (2016).

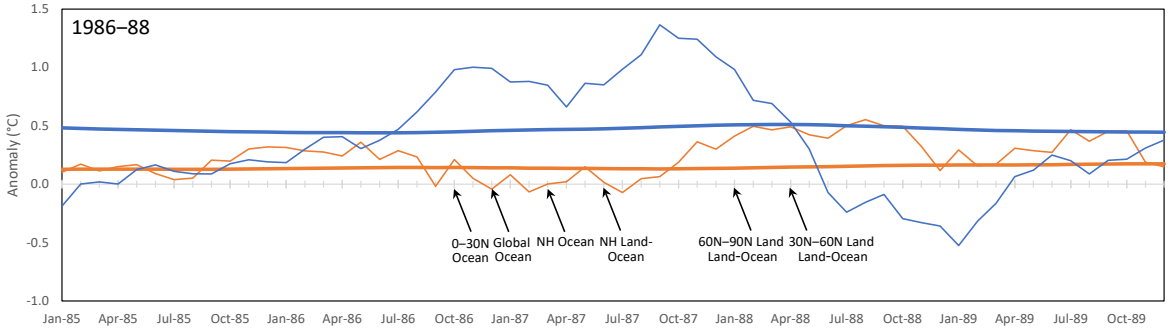

Figure 11 Sequence of shifts 1985–1989, key shown in Figure 8a. Shift timing in Table S8.

The 1995–98 event begins with a shift in the AMO in Mar 1995 and TWP in Apr (Fig. 12). Based on timing, this suggests a teleconnection between the AMO and TWP. Warming progresses to the SH mid latitude ocean by Feb 1996 and land by Aug 1996. In early 1997, NH land shifts warmer under the influence of an El Niño as shown by warmer conditions in TEP. This is followed by warming further north during 1988. The PDO shifts to its negative phase in Jun 1998 with the inception of La Niña conditions.

https://doi.org/10.5194/esd-2021-61
Preprint. Discussion started: 22 July 2021

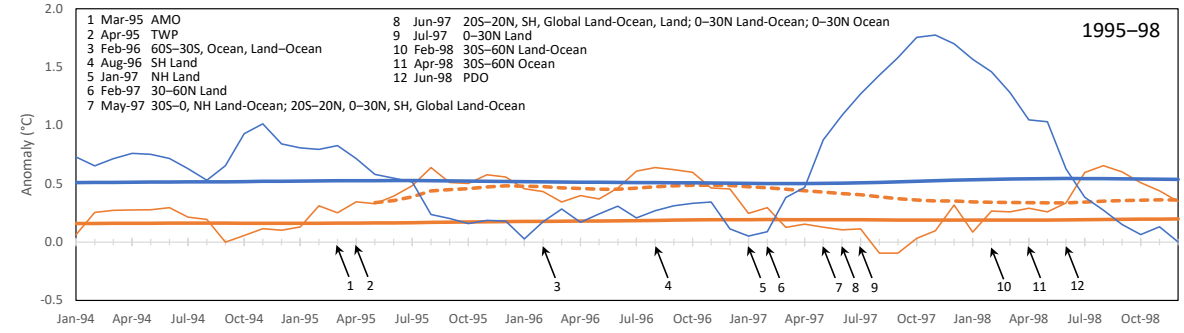

Figure 12 Sequence of shifts 1994–1998, key shown in Figure 8a. Shift timing in Table S8.

A brief 0.2 °C anomaly in the warm pool in Oct 2009 and a longer one during the next year coincides with land-ocean and ocean 60° S–30 °S in Dec 2009. This is associated with shifts in Australian climate (Jones and Ricketts, 2019). This event resembles the 1968 event, where a shift into the SH mid latitudes affecting Australia precede the large 1976/77 shift.

The most recent event begins with a shift in TWP in Dec 2012. The 0.2 °C threshold is exceeded Sep–Oct 2013, Sep 2014–Feb 15 and May 2016–Mar 17 (Fig. 13). Shifts register in mid to high NH latitudes in mid to late 2013, at the hemispheric and global scale for ocean and land-ocean in the first half of 2014 and land in the second half. The PDO shifts positive in Mar 2014 and precedes a potential shift in TEP by a month. In mid-2014, the PDO shifts with a large El Niño cascading through the tropics and southern hemisphere, with shifts in NH and global land registering in Dec 2014.

The increase in temperature 2014–2018 over 1997–2013 in the NCDC record is 0.26 °C globally, 0.17 °C in the SH and 0.34°C in the NH. Allowing for spatial differences, just over half the warming occurs in SST and two-thirds in the NH. In NH latitudinal zones, 00°–30° N and 30° S–60° N rose by 0.31 °C and 60° S–90° N by 0.66 °C. Land temperatures in Europe increase by 0.59 °C.

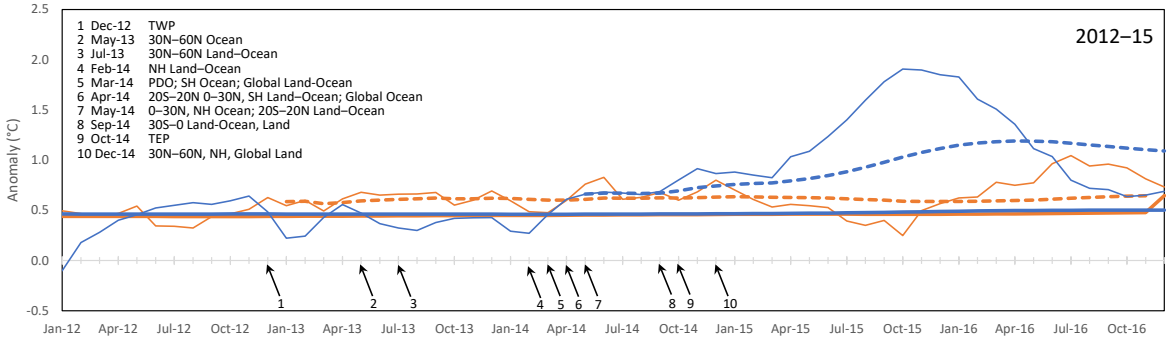

Figure 13 Sequence of shifts 2012–2016, key shown in Figure 8a. Shift timing in Table S8.

These events all show shifts starting in the surface ocean. The three global events 1976–78, 1995–98 and 2012–15 all coincide with changes in decadal oscillations, with El Niño events providing the main source of heat. The sign of phase shift in these oscillations is likely to be important. The PDO shifts positive in 1976, PDO and TEP shifting one month apart. In 2014, the PDO leads TEP by seven months. A positive shift of the AMO in 1995, is followed by a negative shift in the PDO

https://doi.org/10.5194/esd-2021-61
Preprint. Discussion started: 22 July 2021

in June 1998 during a La Niña and the last in that sequence. Decadal oscillations becoming unstable during a regime shifts could potentially provide kinetic energy contributing to the emplacement of warmer regimes.

Whether TWP represents a thermostat or not is unclear from this analysis. TWP shows a build-up of excess heat during events, but is barely present in the 1976–77 sequence, then precedes a second round of warming in 1978–79. The 0.2 °C threshold is exceeded for an extended period in 1988, but TWP does not undergo a regime shift, although cooling due the Mt Pinatubo eruption in 1991 may have prevented that. Excess heat in TWP precedes the El Niño event in 2014–15, followed by warming in the NH during 2013.

3.3 Tracking changes in teleconnections

This section addresses the relationship between decadal oscillations, heat engine behaviour and regime shifts. Globally, the interactions between patterns of SST across different ocean basins form a "network of teleconnections (Cassou et al., 2018)". Teleconnection behaviour and radiatively-forced climate change are generally considered to be independent processes, but interactions between the two, particularly external forcing influencing variability, are increasingly being considered (Cassou et al., 2018), conclusively by some (Wu et al., 2019).

Whether the AMO and PDO are 'true' oscillations is sometimes questioned due to a perceived lack of periodicity (Cassou et al., 2018). Moreover, beyond the patterns defining the indices lie a more complex set of mechanisms described as Atlantic Multidecadal Variability (AMV) and Pacific Decadal Variability (PDV) (Newman et al., 2016;Cassou et al., 2018;Wu et al., 2019;Johnson et al., 2020a). Understanding the internally-generated contributions to these is a requirement for separating variability from the forced signal as part of predicting the future evolution of climate (Wu et al., 2019). While the standard method does so by assuming an underlying gradual change proportional to forcing, we focus on regime-like behaviour in decadal oscillations and their potential teleconnections.

3.3.1 Pacific Decadal Oscillation

We report on how the PDO index interacts with the Pacific Ocean heat engine (data sources described in the SI). The main index used is the EOF of detrended monthly Pacific SST poleward of 20 °N 1900–1993 (Mantua et al., 1997;Hare and Mantua, 2001), compiled from ERSSTv5 (Huang et al., 2017). Although PDO was originally associated with the northern Pacific (Mantua and Hare, 2002;Newman et al., 2003), Newman et al. (2016) recognise tropical and north Pacific components. A separate Southern Decadal Pacific Oscillation (SPDO) has also been recognised (Hsu and Chen, 2011;Chen and Wallace, 2015). The Interdecadal Pacific Oscillation (IPO)(Power et al., 1999;Henley et al., 2015) combines three nodes in the north, central and south Pacific. This is represented by a tripolar IPO index which we tested for regime-like behaviour, finding little, so did not continue with it. This is largely because the behaviour in the north and south nodes is complementary but different – when tropical Pacific forcing is removed, the correlation between these nodes disappears (Zhang et al., 2018). Two climate models driven by Pacific Ocean salinity and temperature anomalies show that the PDO variability is driven by the tropical Pacific (Johnson et al., 2020b).

https://doi.org/10.5194/esd-2021-61
Preprint. Discussion started: 22 July 2021


Earth System Dynamics Discussions

Phase length, mode, anomalies for TEP, TWP, the difference between the two and the change in that difference from the previous period are shown in Table 1. Phases are identified as positive or negative, which represent El Niño-like or La-Niña-like behaviour in the tropical Pacific. Based on the direction of regime change, these are interpreted as two positive phases 1896–1946, negative to 1975, positive to 1998, negative to 2013 and positive from 2014.

Table 1 PDO phase, period, temperature anomalies in TEP and TWP, difference between TEP and TWP, change in difference and length of phase.

Period	Length (y)	PDO phase	TEP anom (°C)	TWP anom (°C)	TEP-TWP (°C)	δTEP-TWP (°C)
1880–1895	16+	Negative	-0.08	0.00	2.19	
1896–1924	29	Positive	0.05	-0.26	1.81	0.37
1925–1946	22	Positive	0.17	-0.13	1.84	-0.02
1947–1975	29	Negative	0.08	-0.05	1.99	-0.15
1976–1998	22	Positive	0.57	0.17	1.77	0.22
1999–2013	15	Negative	0.39	0.47	2.23	-0.46
2014–2018	5+	Positive	0.92	0.70	1.93	0.30

Phase lengths show two alternating sets of 29 and 22 years followed by a negative 15-year phase 1999–2013, truncated from 29 years if the same pattern had been repeated. Shorter phase lengths and a stronger signal may be a response to forcing, as analysed for observations and the 21st century (Bonfils and Santer, 2011;Dong et al., 2014). The phase changes between periods in Table 1 register as shifts with p values decreasing over time from three PDO indices (Table S5), are consistent with the PDO responding to external forcing. Zhang et al. (2018) reproduce the regime shifts of 1947, 1976 and 1998 in a pacemaker experiment where the tropical Pacific is used to force the ocean.

Phase changes in the PDO since the 1970s have been associated with increases in TWP of 0.2 °C to 0.3 °C (in 1978, 1997 and 2014). Shifts in the NH in 1925–26 and globally in 1976–77 and 2013–14 coincided with shifts in PDO from negative to positive phase. Most warming since 1880 has taken place during positive phases, consistent with the standard explanation based on trend analysis (Folland et al., 2018). Since 1880, PDO was positive 57% of the time for 80% of total warming, negative for 43% of the time for 20% of total warming. Most of this warming has occurred as shifts (93%) compared to trends.

The TWP-TEP temperature gradient of 1.94 °C is ≥2 °C for negative phases (La Niña-dominated) and <1.9 °C for positive phases (El Niño-dominated). It is inversely correlated with the PDO Index (-0.62, $p=4.8 \times 10^{-16}$, Fig. 14). These differences in gradient are mainly due to variations in TEP, which cool slightly for each positive phase-shift, and warm for each negative shift. For the last two positive phase shifts, TEP increased by ~0.46 °C, compared to the earlier changes in 1896 and 1925 of 0.13 °C and 0.12 °C, respectively.

https://doi.org/10.5194/esd-2021-61
Preprint. Discussion started: 22 July 2021

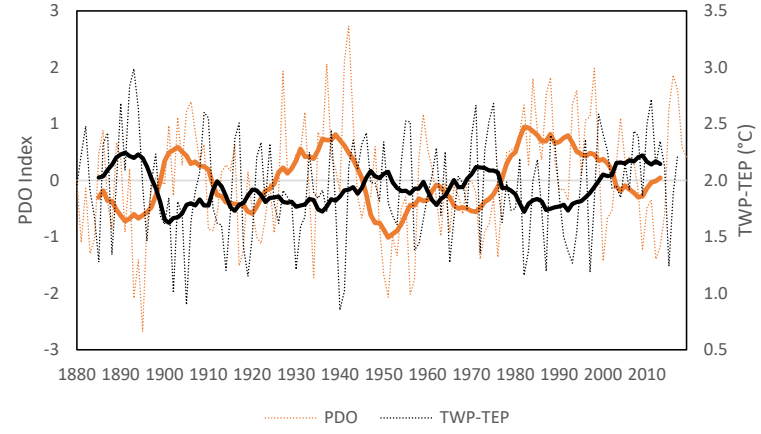

Figure 14 Comparison of the PDO Index and TWP-TEP difference shown with 11-year running means.

A comparison of Figs. 4 and 14 shows TWP moving in smaller, more frequent steps and TEP in larger, infrequent steps (Fig. 4) while maintaining a dynamic relationship with the TWP-TEP gradient (Fig. 14). The three times the 11-year running mean of the gradient has exceeded ~2.1 °C, TWP has either decreased (1901) or TEP increased (1976, 2014). The gradient increased to 2.08 °C in 1947, which also coincides with a regime change, but this may be due data quality issues.

The positive and negative PDO phases oscillate between subsurface and meridional transport of heat and atmospheric zonal transport (Zhang et al., 2009;Allen and Amaya, 2018). During its negative phase, TEP is cooler, the intake area of cooler upwelling water from the southern hemisphere wider, and more heat is moved outwards and downwards and less into the warm pool and the TWP-TEP gradient is ≥2 °C. When positive, TEP is warmer and gradient <2 °C, the intake area is narrower, convection enhanced and meridional transport reduced, and the area channelling heat into the warm pool is narrower which receives more heat (Zhang et al., 2009;Allen and Amaya, 2018).

3.3.2 Atlantic Multidecadal Oscillation

The AMO is a see-saw of warm and cool temperatures centred on the NH Atlantic Ocean that undergoes quasi-periodic oscillations and is linked to widespread impacts across the globe (Enfield et al., 2001;Knight et al., 2005;Knight et al., 2006). The AMO Index is based on the detrended SST of the North Atlantic Ocean (Trenberth and Shea, 2006), but until the late 1990s, detrending has a limited effect. Figure 16a compares the Kaplan AMO index (Enfield et al., 2001) to Atlantic Ocean SST for 40–60° N (ERSTTv5), showing that only after 1997, do they differ markedly. Shift detection reveals warm periods 1854–1901, 1926–1962 and 1995 to the present and cool periods from 1902–1925 and 1963–1994. The same periods are recognised by Alheit et al. (2019). All shifts in the AMO are $p<0.01$ with the test statistic not changing markedly over time (Table S6) indicating that the strength of phase changes is not influenced by external forcing. Positive shifts are slightly more than double the size of negative shifts. The timing of shifts with volcanic eruptions show that during the 20th century

https://doi.org/10.5194/esd-2021-61
Preprint. Discussion started: 22 July 2021

Earth System Dynamics Discussions
Open Access
EGU

the AMO has preceded eruptions (Section S3.3), so the volcanic forcing hypothesis prompting shifts to negative phases (Swingedouw et al., 2017;Birkel et al., 2018) does not seem to hold.

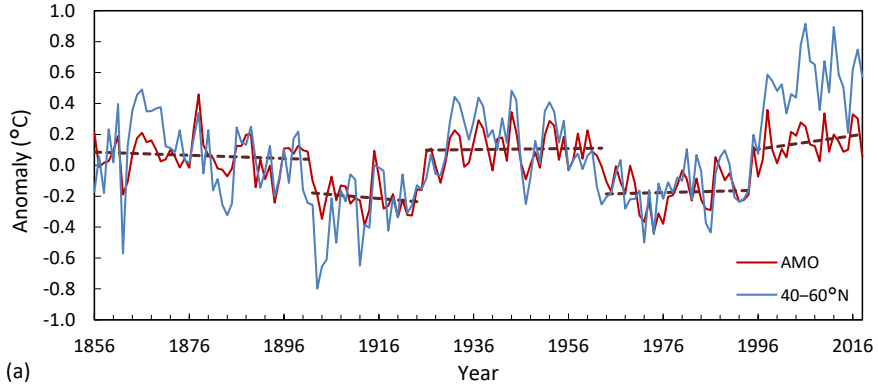

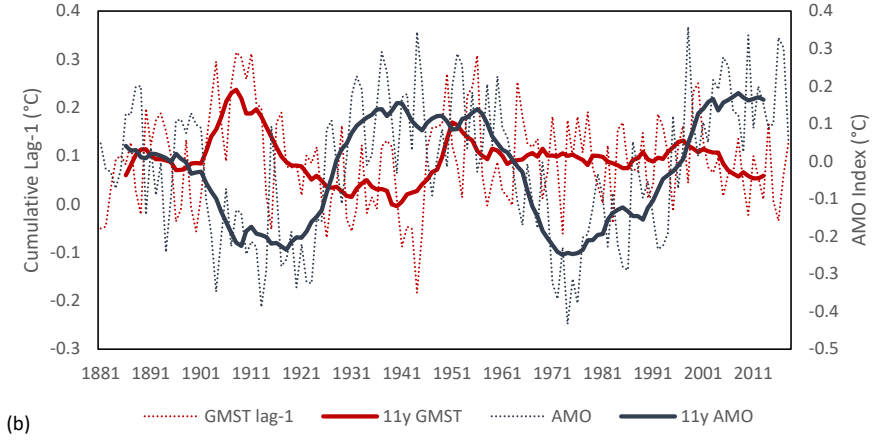

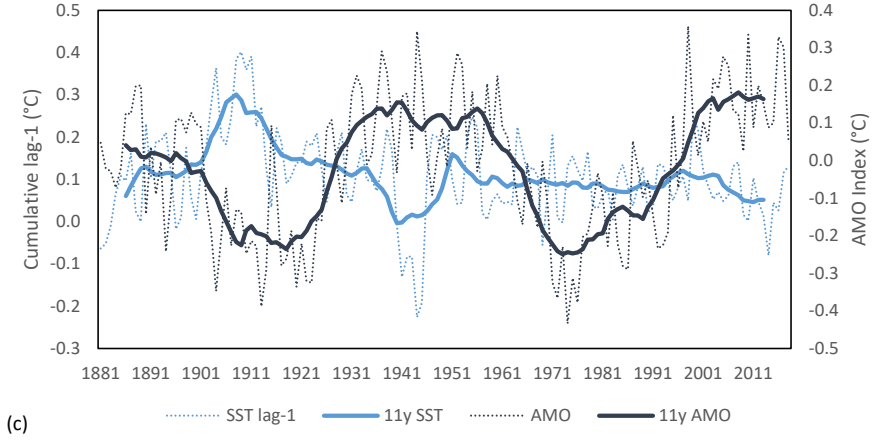

Figure 15(a) Comparison of the Kaplan AMO index with ERSTTv5 SST for 40–60 °N Atlantic Basin, showing annual data and 11-year means; (b) comparison of cumulative lag-1 differences in GMST with steps removed with the AMO index 1881–2018; (c) as for (b) but for SST.

https://doi.org/10.5194/esd-2021-61
Preprint. Discussion started: 22 July 2021

Most shifts in AMO phases follow shifts in global temperature except that in 1963, which is associated with negative shifts in the Atlantic Basin, and 1995, which precedes the shift in TWP by one month, beginning the 1995–98 sequence. According to Sun et al. (2017) this was a direct influence. Comparing Fig. 15b with Fig. 7b shows that the redness in GMST is due to the AMO and in Fig. 15c this mainly influences the ocean component before both records whiten as shown in Fig. 7.

The 1995 positive AMO shift has been widely documented as a regime shift (Gray et al., 2003;McCabe et al., 2004;Enfield and Cid-Serrano, 2006;Alheit et al., 2014), rising by over 1 °C in two years (Robson et al., 2012) accompanied by rapid changes in ocean heat content (Ishii and Kimoto, 2009;Levitus et al., 2009). The Atlantic and Pacific decadal modes have been linked on the basis of cross-correlations suggesting leads and lags of multiple years (d'Orgeville and Peltier, 2007;Zhang and Delworth, 2007). This is not supported by the Granger analysis presenting in Sect. 3.4. Lagged autocorrelations suggest repeating patterns in each and between them but not cause and effect.

Interbasin connections between the Atlantic and Pacific are becoming better understood. Sun et al. (2017) compared the detrended N part of the warm pool with the N Atlantic Ocean 0–60° N 1900–2013 finding a correlation of 0.68. They ran a pacemaker experiment of the Atlantic sector in a slab ocean model to determine the effect on the Pacific, identifying an atmospheric bridge into the central north Pacific and an area of convergence on the surface in the western Pacific, divergence in the east and the opposite in the upper atmosphere, consistent with increased east to west airflow and warmer TWP (Sun et al., 2017). They interpret this as an influence on TWP decadal variability. To see whether increasing teleconnections may also influence regime shifts, we removed steps from the northern half of TWP and the stationary Atlantic region 0–60° N with data from ERSSTv5; their correlation is 0.15 in free mode and 0.45 in forced mode ($p=0.15$ to 0.001). Correlations with the southern half of the warm pool are slightly weaker. The links between the Pacific and Atlantic therefore strengthen with forcing.

3.3.3 Atlantic Meridional Overturning Circulation

The AMOC is the slowest of the climate modes investigated. The main questions are whether it shows regime-like behaviour and is linked to the larger climate network. The recent slowing of the AMOC has been attributed by some to external forcing (Rahmstorf et al., 2015;Caesar et al., 2018). Opinions differ as to whether AMOC responds to internal and external forcing in a regime-like way, or smoothly (Wunsch and Heimbach, 2013).

The AMOC Index 1871–2016 constructed from HadISST (Caesar et al., 2018) shifts down in 1969 by -0.60, up by 0.38 in 1997 and down by -0.74 in 2014, the latter mirroring phase shifts in the PDO (all $p<0.01$). The associated Gulf Stream Index undergoes a positive shift in 1944 and negative shift in 1956 – it is unclear to whether this is a short-term excursion or an inhomogeneity. It undergoes another positive shift in 2011. The two records diverge markedly in 1972, having tracked closely beforehand.

Two similar SST indices have been used to trace AMOC back to just before 1000 AD, showing increases from 1500 to 1800, a slight decrease in the 19th century, before those noted above (Rahmstorf et al., 2015;Caesar et al., 2018). Thornalley et al.

https://doi.org/10.5194/esd-2021-61
Preprint. Discussion started: 22 July 2021


Earth System Dynamics Discussions

(2018), using proxies in the Baltic Sea conclude that the AMOC has been weakened for the past 150 years compared to the preceding 1,500 and the transition may have been abrupt.

Dima and Lohmann (2010) identify two modes in Atlantic deep-water formation, a slow mode decreasing gradually since the late 1930s and a fast mode shifting negative and positive around 1970 and in the late 1990s. AMOC is generally seen as influencing the AMO (Marini and Frankignoul, 2014;Zhang et al., 2019) but two-way oscillatory relationships have been observed in model studies (Kim et al., 2021) including CMIP5 models (Zhang and Wang, 2013). The recent changes in a range of surface variables that show a relationship between Atlantic multidecadal variability and AMOC are consistent with recent direct estimates of AMOC flow volumes (Sun et al., 2021). The stability of AMOC is very much a matter of debate, but simple and intermediate models produce abrupt phase transitions (Dijkstra, 2019;Johnson et al., 2019), while more complex models produce a wide range of responses, showing high sensitivity to the background state (Johnson et al., 2019).

3.4 Granger analyses

Granger analysis can potentially identify delayed influences in a flow system, so the 29 NCDC temperature records were analysed in pairs to determine what influence they have on each other. The full analysis involves monthly deseasonalised and annual data, stationary (steps removed) and observed data for free and forced periods and two-way analysis between pairs. This generates a large amount of data (16 sets) so only the results of most interest are summarised here. Correlations and lagged correlations provide additional information. In the following descriptions the stationary data 1880–1967 is nominated as FreeS, nonstationary data Free+, stationary data 1968–2018 ForcedS and nonstationary data Forced+. Technical descriptions, a guide to interpreting the results and additional results are provided in the SI.

The stationary data lies within the design parameters for the test, whereas the nonstationary does not. Stationary data represents climate in steady state. P-values are only used to determine which variables may have influence on an annual basis. Due to high sample numbers, f-stat value for the forced period are low (n=612, p0.05=0.08, p0.01=0.10) and the free period slightly lower so have little meaning. The most important results come from comparing stationary and nonstationary results to determine which variables have the most influence and how they change. From that we can gain an understanding of flow relationships during shifts. F-stat results up to lag-24 are calculated where possible and are limited to lag-15 for annual data 1968–2018.

The correlation matrices for stationary data show changing connectivity between free and forced modes. Correlations are considered only for stationary data, because they reflect circulation patterns, whereas observations are dominated by warming. Monthly correlations for global land show the influence of NH land whereas the global ocean is mainly influenced by the tropical ocean. TEP has a correlation pattern typical of ocean regions whereas TWP is poorly correlated. From free to forced modes, ocean regions become slightly less correlated and TEP and TWP become slightly anticorrelated (Table S10).

For annual correlations during free mode, both global land and ocean correlations are highest for the tropics, hemisphere averages lower and extratropics the least. TEP is typical of ocean regions and TWP shows little correlation with other regions. The decrease for all regions from free to forced mode is larger. Some regions become slightly anticorrelated,

https://doi.org/10.5194/esd-2021-61
Preprint. Discussion started: 22 July 2021


Earth System Dynamics Discussions

including TWP and TEP (just outside the p=0.05 level). The most independent regions are 30–60° S, TWP and 60–90° N (60–90° S is excluded; Table S11.

Monthly Granger influences to land, ocean and GMST are generally lag-1 tapering quickly, meaning the that last month from the incoming region influences this month's temperature and that influence does not last. For global land, influence from other regions is minimal in the FreeS period, increasing markedly throughout the sequence Free+, ForcedS and Forced+. Influences to land are widespread, dominated by global mean SST and GMST during Forced+, showing the land receives heat from all regions during shifts.

Influences to global SST are quite different, being larger for stationary timeseries and increasing from free to forced periods. TWP and TWP are the main influences, with a strong lag-1 effect, with a declining but sustained influence to lag-24. TWP and TEP therefore have the largest effect of all regions on monthly global SST during stable periods. During forcing, those influences are suppressed in the first few months but resume their ongoing influence afterwards. This implies a continuous influence via circulation that is interrupted during regime shifts. The tropical ocean has a similar but lesser effect on the wider ocean throughout all periods. Lagged correlations show a transition from positive to negative influences over several months, showing strong negative feedback. This shows that circulation influences a generally short-lived as SST returns to steady-state conditions.

3.4.1 Monthly Granger results

Monthly influences on GMST show a large lag-1 influence from land dominated by NH land and NH extratropics with no input from the tropics or SH land. Ocean influences are almost as large, dominated by the tropics during FreeS before global influences become more prominent through the next three series, although the NH extratropics continue to have little influence. Land-ocean areas have a lesser influence expanding from the tropics to all regions over time, although TEP has a declining influence and TWP none. Redistribution effects and surface feedbacks are the main influences. The period of least influence for this sequence is in forced stationary mode, presumably because the tight coupling of the climate leads more concentrated circulation patterns. Much of this more concentrated circulation moves through the heat engine.

TWP is influenced by lag-1 effects that are minimal in FreeS, influenced by tropical land and ocean regions through Free+, slightly more by tropical lands and the global and NH ocean in ForcedS and strongly by land and ocean regions in Forced+. This reflects the increasing circulation of heat from both land and ocean through the central Pacific to the warm pool. TWP's influence on ocean regions is strongest in ForcedS, less in FreeS and is suppressed during warming periods. For land it is the opposite, with a substantial influence during Forced+. TWP therefore influences the ocean during steady state and the land during warming shifts, the emphasis changing from advection in the ocean to convection.

The tropical ocean influences TEP at lag-3 and TWP at lag-1 for both FreeS and Free+ periods, being unaffected otherwise. In forced mode, these influences are both strong lag-1 and are largest in steady state while also being influence by tropical lands and ocean regions led by the SH at lag-1. Under warming there is little influence, except for the tropical oceans biased south and TWP, suggesting TEP is forcing other regions. Monthly TEP strongly influences other regions, more so in

https://doi.org/10.5194/esd-2021-61
Preprint. Discussion started: 22 July 2021

stationary conditions and stronger in ForcedS, and slightly less in nonstationary conditions. Tropical land regions are influenced in all cases, and all ocean regions except the high latitudes in stationary conditions and restricted to the tropics in nonstationary conditions. The influences on land are likely to be via convection. The reduced influence during warming sequences, is probably because of the involvement of TEP in El Niño events.

The overall pattern sees the climate system becoming more integrated and circulating faster from free and forced mode. TWP and TEP have a profound effect on the ocean, but during warming events the ocean is doing most of the thermodynamic forcing at the monthly timescale. The integration of land and ocean into GMST is an ongoing process of recirculation and feedback redistributing energy (e.g., the hydrological cycle on land and freshwater to the ocean) but the ocean and land form the basic thermodynamic units. Both TWP and TEP show evidence of a change from regional circulation to being more tightly coupled within the heat engine structure, especially during regime changes. The strong negative feedback and return to steady-state on the monthly timescale, suggests that the monthly and interannual relationships can be considered separately.

3.4.2 Annual Granger results

The annual analyses clearly show ENSO as the major driver of lag effects. Decreasing correlations between FreeS and ForcedS show the increasing importance of teleconnections and this is reflected in the nonstationary responses. Fig. 16 compares the major influences to and from global ocean and land, GMST, TWP and TEP. They are compared with the p0.01 threshold, which is applicable to the stationary data. If the results are within that limit, any effects are minor to negligible. The left side of each chart shows the influence coming in from each of the regions shown and the right side the influence from global ocean, land or land-ocean. The difference between the stationary and nonstationary results shows the influence of shifts.

Before 1967, most influences are relatively weak even during regime shifts. Some regional influences are not included (see the SI) but are minor. Influences on global ocean to 1967 are largely limited to lag-1 influence from tropical lands in FreeS and tropical ocean in Free+. From 1968, TEP with a lag-2 peak dominates both cases, with the central tropical ocean almost as strong. Tropical land continues to have a lag-1 influence for Forced+. Annual influences on global land to 1967 are negligible as is the case for GMST. Under stationary conditions, there is a lag-2 influence from TEP and the tropical ocean. Warming is driven by are strong lag-1 influences from the NH and GMST and lag-2 influences from TEP and the tropical ocean. From 1968, TEP is the principal influence on GMST. For stationary conditions, the largest input is from TEP at lag-3 followed by the tropical ocean at lag-4, showing the ENSO 2–7-year frequency. Under warming, TEP is strongest at lag-2, followed by NH, global and tropical oceans, global, NH and high latitude land.

For TWP, The NH, tropics and GMST have a minor influence to 1967, strengthening slightly in response to regime changes, which also contains a small lag-2 peak. This is not directly due to TEP which has a small lag-1 effect but is referred. TEP has a lag-2 effect on tropical land and ocean at the same time. From 1968, TWP is relatively autonomous in stationary conditions as indicated by its low correlation with other regions. However, under regime change it is highly influenced by other regions

https://doi.org/10.5194/esd-2021-61
Preprint. Discussion started: 22 July 2021

Earth System Dynamics
Discussions
Open Access
EGU

on a sustained lag-1 basis. It also projects a small referred influence to the tropical ocean and other regions. This is interpreted as heat from the warm pool feeding into El Niño events, hence referred rather than direct. As described above, TEP shows lags 3–7 and lag-2 with the largest impact on tropical land.

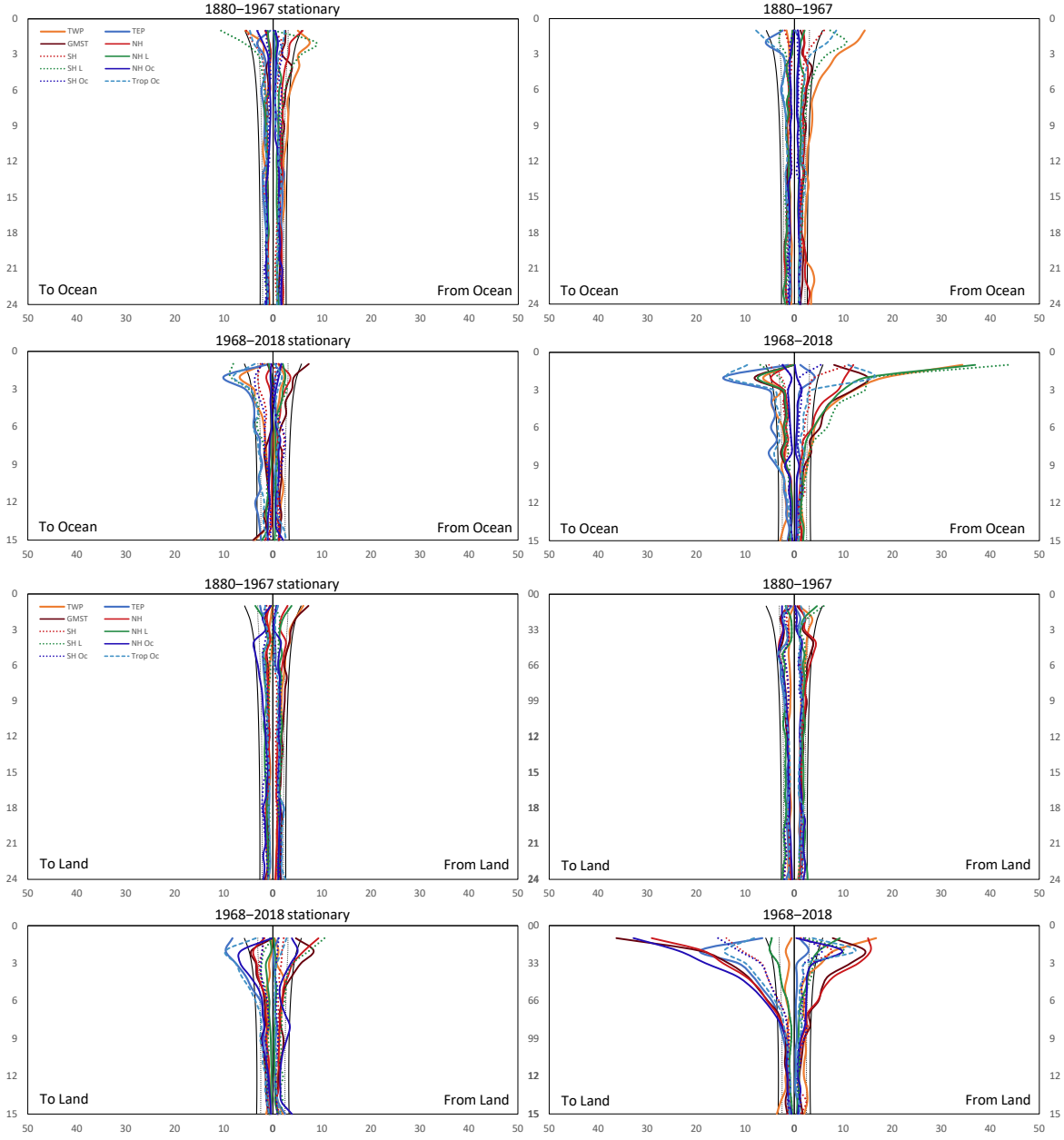

https://doi.org/10.5194/esd-2021-61
Preprint. Discussion started: 22 July 2021

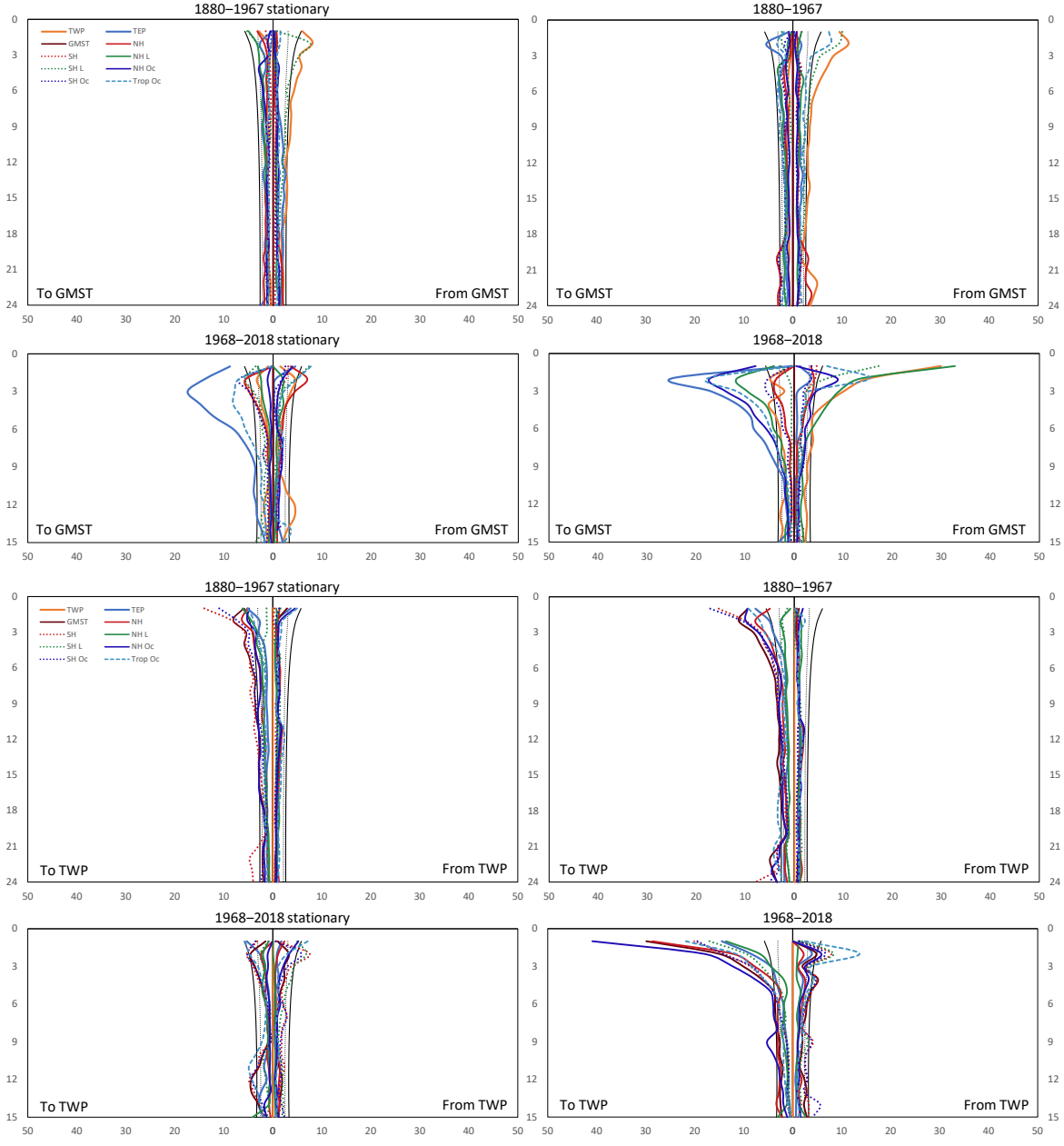

645

https://doi.org/10.5194/esd-2021-61
Preprint. Discussion started: 22 July 2021

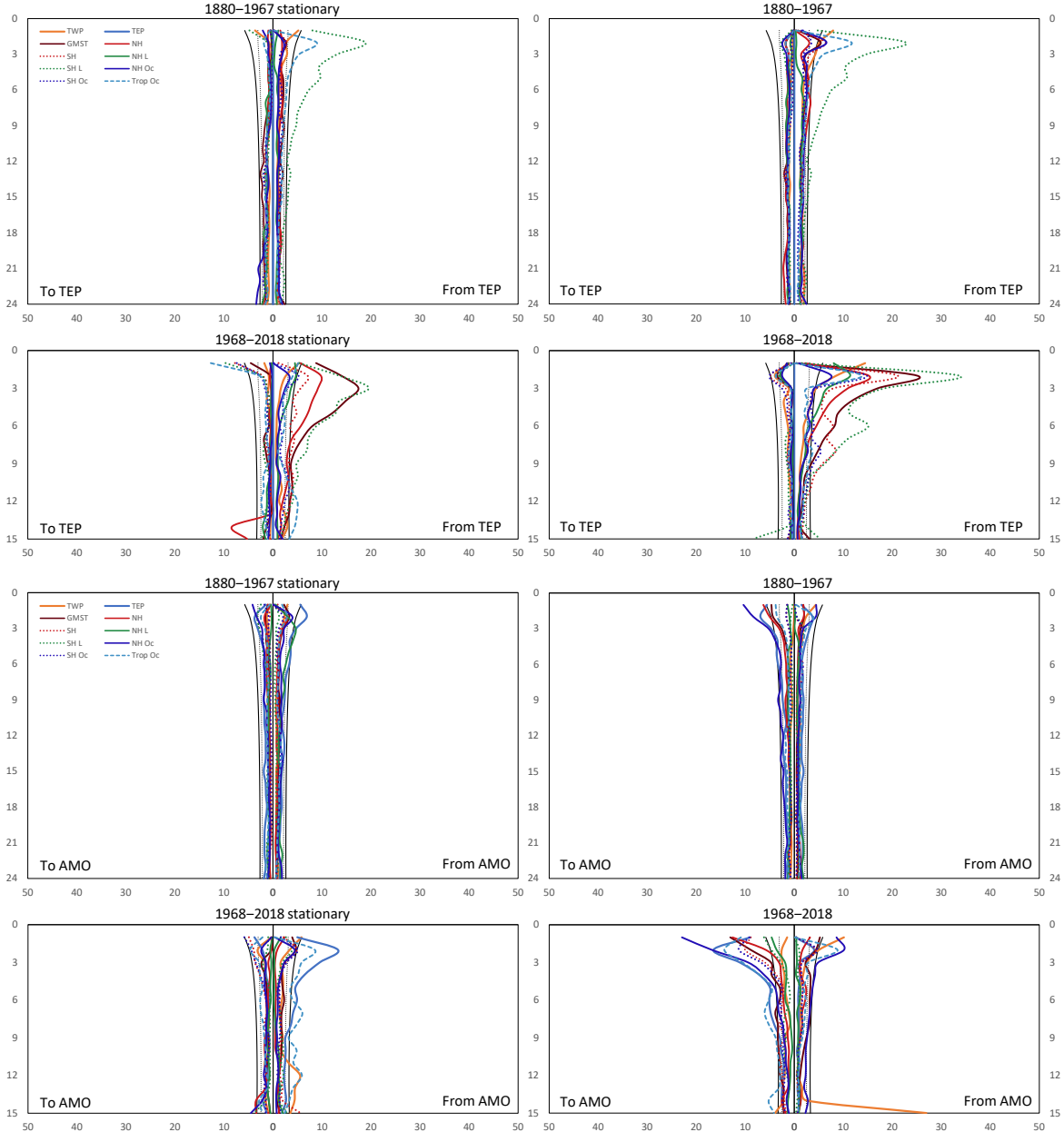

Figure 16 Results of Granger analyses (f-statistic) for global ocean, global land, GMST, TWP, TEP and AMO showing 1800–1967 stationary and nonstationary data followed by 1960–2018 stationary and nonstationary data. The solid black lines are the p0.01 threshold, but are only valid for the stationary data.

Together, they show that from 1968 TEP is the major vehicle for warming. Heat from El Niño events flows back through the heat engine in the following year showing up as lag-1 influences on TWP and the contribution of both latent and sensible heat from land (as freshwater) produces a sustained input. The El Niño event from TEP is remembered by the system but when it returns to TWP in the follow year, TEP retains no record of its passing. Using a heat engine metaphor, TWP is acting

https://doi.org/10.5194/esd-2021-61
Preprint. Discussion started: 22 July 2021

like the boiler, storing heat up to a constant limit and boiling it off as convection, while also leaking in all directions (meridional transport in the shallow ocean, to the Indian Ocean and in return flows), while TEP, despite being cold, is the furnace, which retains little memory of the heat transferring through. When the system reaches a critical point of release, the furnace releases a large amount of heat.

During shifts from 1968, the direction of flow is overwhelmingly from ocean to land. On a monthly basis, the ocean has a very strong lag-1 influence on land regions, affecting the tropics, global and hemispheres and extratropics in that order. There is limited redistribution within the ocean, but land shows a strong redistribution from tropical to higher latitude land, as does TWP, showing enhanced convection during regime shifts. For the ocean, 60–90 °N is the exception, being influenced by both ocean and land. On an annual basis, the direction is also principally from ocean to land, but recirculation also produces smaller knock-on effects from land, eventually flowing back to TWP.

Before 1968, most regime shifts affected the northern mid-latitudes and tropics with heat dissipating via limited circulation and limited teleconnections. From 1968, regime changes became global with increased teleconnection and TEP becoming the main source of the heat for regime shifts. However, this analysis does not reveal what causes regime shifts, or whether either TWP or the relationship between TWP and TEP is acting as a thermostat.

Additional analyses were conducted on the AMO and PDO to see whether they are responding to regime shifts or contributing to them in any way. The PDO shows very little interaction with other regions except for minor input and effects on tropical lands. The only exception is the stationary record in forced mode, where a number of regions show a strong influence from the PDO at lag-14–15 and a similar influence to the PDO in the nonstationary record. This is probably picking up two successive shifts where the PDO is involved in 1998 and 2014.

The NH ocean has some lag-1 influence and TEP lag-2 influence on the AMO during Free+, but during Forced+ the NH and N and S tropical oceans, and tropical lands have a lag-1 influence and TEP and central tropical ocean a lag-2 influence (Fig. 17). For the influence of the AMO on other areas the AMO has a small lag-2 influence on TEP during FreeS and on the 0–30° N ocean during Free+. During the ForcedS period, the AMO has a stronger lag-2 influence on TEP, 0–30° N and central Pacific Ocean and minor lag-1 influence on land. During the Forced+ period there is a strong lag-2 effect led by the NH and other ocean regions and an equivalent lag-1 effect on TWP.

This suggests the AMO is communicating with TEP on a lag-2 delay during stationary periods in forced mode and TEP is forcing the AMO lag-2 while the AMO is having a lag-2 effect on mainly NH and tropical oceans while also feeding back to the warm pool one year later. Atlantic-Pacific linkages are being increasingly recognised (Dong et al., 2006;Yu et al., 2015;Park and Li, 2019;Johnson et al., 2020b), so this warrants further investigation.

3.4.3 Relationship between TEP, TWP and broader climate

The relationship between TWP and TEP reveals interesting dynamics. Figs 17a and b show the Granger results for the monthly influence between the two for the free and forced periods, and Figs 17c and d the corresponding lagged correlations. TWP influences TEP lag-1 to 1967, lag-3 during warming from 1968. Lagged correlations are lens-shaped, the lag-12

https://doi.org/10.5194/esd-2021-61
Preprint. Discussion started: 22 July 2021


Earth System Dynamics Discussions

influence of TEP on TWP is positive and lag 3–6 effect of TWP on TEP. This may represent flow of cooler water from TEP to TWP, and return flows of warmer water to TEP producing a negative feedback. This is consistent with satellite sea level data from Niño 3.4 and the Indonesian region, which has leads, lags and parity between the two on monthly timescales, suggesting oscillatory behaviour on sub-annual and interannual timescales. For annual data, the influence is greater from TEP to TWP, stronger during nonstationary episodes (Figs 17e–f). TWP and TEP show an interacting opposing-phase relationship, which becomes more distinct during forced mode. The annual lagged correlations for stationary data (Figs 18g–h) show clear reversals. The pre- and post-1968 data suggest that coupling between the two is weak before 1968 and stronger afterwards, as the reversals become more distinct. These correlations are swamped in the warming case.

Fig. 18 shows the influence of TWP and TEP on GMST. The ENSO cycle of 3–7 years for the stationary data (Fig. 18a) and strong 2-year lag for the nonstationary data in Fig. 17 is repeated (Fig. 18b). TEP-TWP lagged correlations with GMST from 1968 show a similar structure to the TWP-TEP relationship. This is also the case for global ocean and land, with ocean having sharper reversals. The correlation between the lagged correlations between TWP-TEP and TEP-Ocean during the forced period is -0.65 ($p<0.01$), and between TEP-TWP and TWP-GMST is the same (-0.65), both for stationary data. However, the preceding year's TWP-TEP relationship between TEP-GMST is 0.56 ($p<0.05$) and the following year's is -0.85 ($p<0.01$). This is consistent with TWP-TEP acting like a recharge-discharge oscillator, where a positive/negative relationship between TWP and TEP is followed by one of the same sign between TEP and GMST and the following year the TWP-TEP relationship is of the opposite sign. Because both the land and ocean are in phase with GMST, they also share this relationship. From 1968, the lag-2 correlation in the stationary data between TEP and the ocean is -0.65 ($p<0.01$), with GMST is -0.46 ($p<0.01$) and land is -0.29 ($p<0.05$).

Therefore, the oscillatory behaviour involving TWP and TEP is also reflected in the relationship between TEP and the broader climate system. This relationship is strongest with the ocean, which in turn affects the land and land-ocean records. It does not indicate regime shifts. Removing steps from the data removes the following regime mean but does not remove the El Niño event, which is represented in the stationary data.

Testing lagged correlations and taking the differences between individual years, confirms that when a lag-2 event is initiated, the resulting changes are recorded at lag-1 and lag-0. A lag-1 event is initiated in the timestep before it is observed. To understand how well the test detects steps, experiments with randomised data containing lag-2 shifts failed to represent them, detecting only lag-1. However, when steps or a simple trend is added to stationary TEP data it produces a lag-2 peak when tested on itself using a 1-year lag. This works for tropical ocean SST, but not extratropical SST, TWP or land. The lag-2 peak was also produced on a 2-year auto-lag with the addition of more complex data. Adding complexity produces more attenuated results (e.g., by adding autocorrelation and additional lags). This shows that the test is recognising oscillatory behaviour as in Figs 17 and 18. Shifts need to be identified independently.

Figure 17 Granger test results for monthly TWP – TEP pairs stationary (a) and observed (b) for free and forced periods, and related lag-correlations; (c, d); annual TWP – TEP pairs stationary (e) and observed (f) for free and forced periods, and related lag-correlations for the first fifteen years (g, h). Annual correlations p0.05=0.21 and p0.01=0.27 to 1967; 0.27 and 0.35 from 1968.

https://doi.org/10.5194/esd-2021-61
Preprint. Discussion started: 22 July 2021

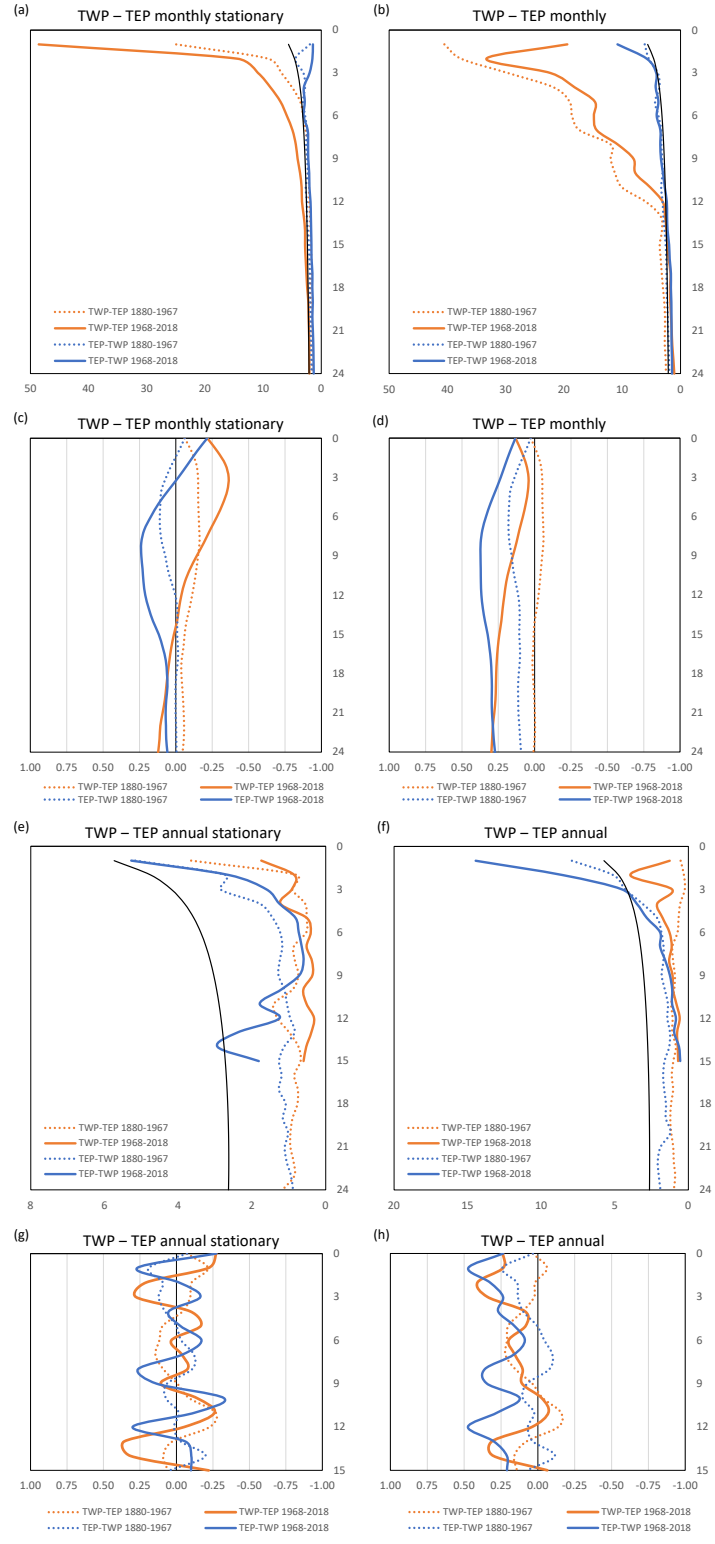

https://doi.org/10.5194/esd-2021-61
Preprint. Discussion started: 22 July 2021

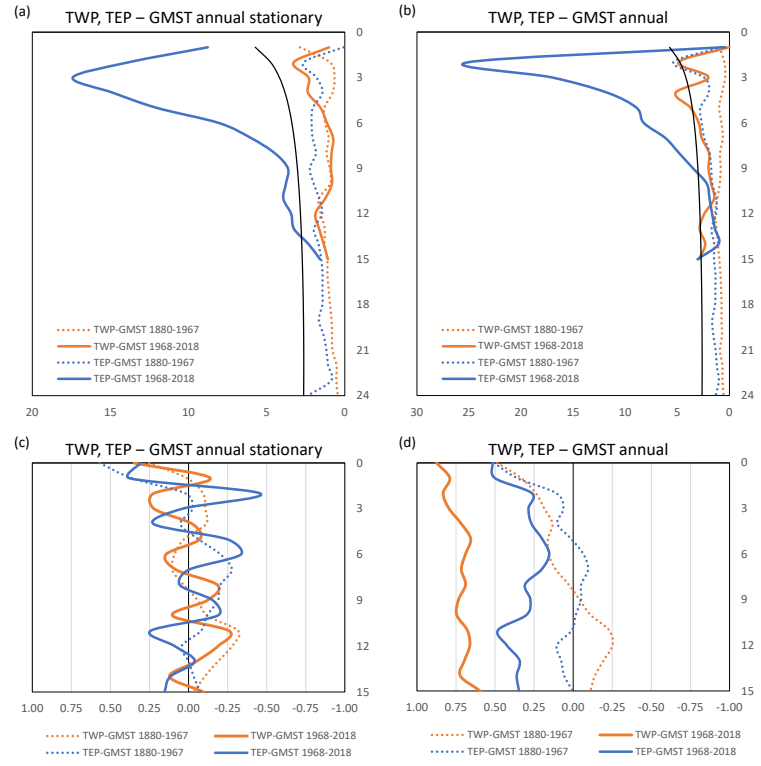

Figure 18 Granger test results for annual TWP, TEP – GMST pairs stationary (a) and observed (b) for free and forced periods, and related lag-correlations for the first fifteen years (c, d).

The Granger tests show important differences between the free and forced modes of historical climate, which include an evolution from regional to global change, a change from circulation to teleconnection leading to greater integration between regions and cross-hemispheric interactions, an intensification of the ENSO cycle, an increase in oscillating behaviour with the Pacific Ocean heat engine and the central role TEP plays in regime shifts. The intensification of ENSO in the late 20th century relative to pre-industrial periods prompted Timmermann et al. (2018) ask whether its evolution and amplitude are responding to external forcing. Based on these analyses, we see a key role for both the heat engine and ENSO in governing the climatic response to thermodynamic forcing. This topic is pursueed in Paper 2.

3.5 The Pacific Ocean heat engine

The above analyses, informed by additional observations and modelling studies, contribute to an overall picture of the Pacific Ocean heat engine. Fig. 19 outlines the major energetic pathways moving through the heat engine. Kinetic energy brings heat from the east through the Walker Circulation and the Coriolis effect contributing to trade winds. Currents formed from upwelling cold water in the southeast and return waters to the north-east and south-east circulate via subtropical gyres. These fluctuate on seasonal, interannual timescales and decadal timescales, the latter influenced by the PDO.

https://doi.org/10.5194/esd-2021-61
Preprint. Discussion started: 22 July 2021

The reverse structure of the heat engine makes it a natural heat pump with forced convection. Natural heat engines are irreversible (Wheatley et al., 1986), but taking the sum of friction and loss of heat at the boundaries, they become equivalent to reversible engines, the difference being the generation of entropy (Bejan, 2019). Given the incoming kinetic energy and additional downward radiation flux, the maintenance of a constant temperature gradient involves a balance between negative surface feedback, friction and convection while maintaining a constant gradient where losses involve a trade-off in heating and cooling rates. If the incoming work is held constant, the amount of heating/cooling measures the coefficient of performance, which is based on the temperature difference between the reservoirs (Feidt, 2010). The difference is inversely correlated with the PDO, which mainly involves a change in TEP, so the difference is less when TEP is warmer and circulation is more zonal, and larger when TEP is cooler and circulation is more meridional. However, nonlinear boundaries lead to roughly 30% difference to a linear flow and in an irreversible situation, this difference is unknown (Lundqvist and Öhman, 2017).

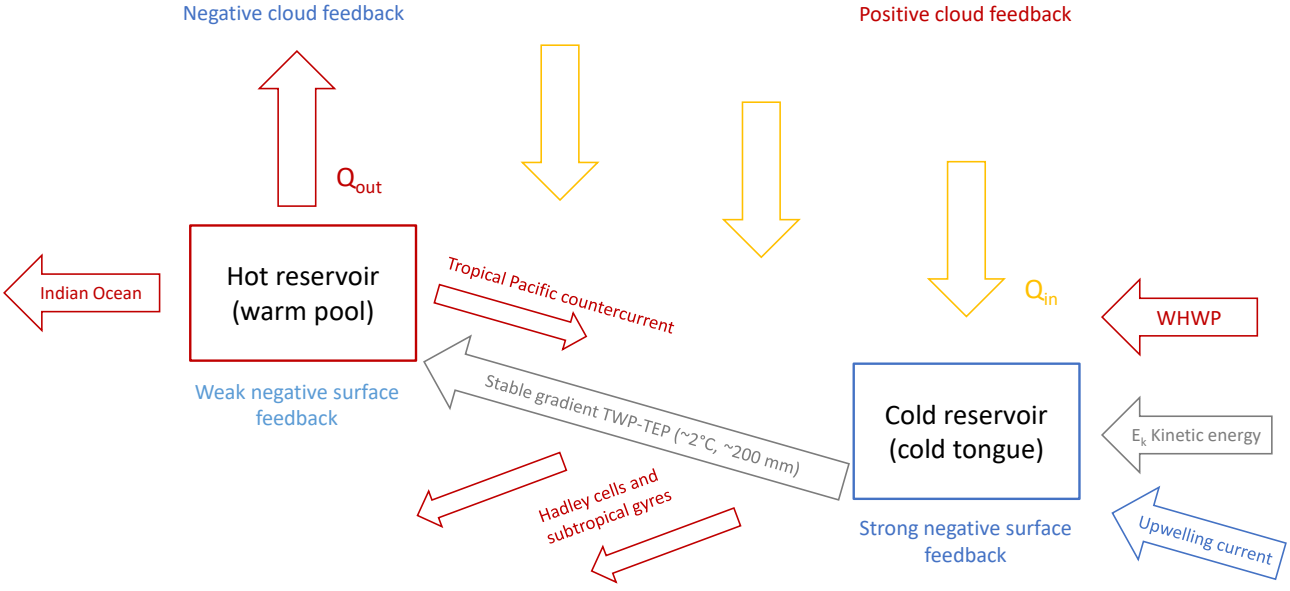

Figure 19 Schematic of the Pacific Ocean heat engine showing kinetic energy (Ek) and power in and out (Q). Red denotes circulating heat, yellow incoming radiation, blue circulating cold and grey, incoming kinetic energy. WHWP is the western hemisphere warm pool.

The warm pool is similar in structure to solar collectors and distillers augmented by a heat pump. Instead of a distiller, heat is delivered into the warm pool where SST above a 28 °C threshold is subject to deep convection (Fu et al., 1994;Sud et al., 1999). Compared to a passive solar collector, a heat pump can be in the vicinity of 50% to 100% more efficient, operating at up to ~90% peak efficiency (Sivakumar and Sundaram, 2013;Yang et al., 2016;Hidouri and Mohanraj, 2019). This figure measures the efficiency of distillation, so differs from the natural heat pump, but demonstrates the benefit of being able to utilise the kinetic energy provided by the Coriolis effect to deliver large amounts of heat for dissipation. Heat pump

https://doi.org/10.5194/esd-2021-61
Preprint. Discussion started: 22 July 2021


Earth System Dynamics Discussions Open Access EGU

performance is affected by pinch points, sites of minimum temperature, so maintaining a constant gradient helps to keep heat engine performance relatively consistent. The reset mechanism provided by changes between multiple cycles, counterbalanced by the strong negative feedback centred on TEP and weaker feedback in TEP and the exchange between TWP and TEP, allows continual opportunity to keep the engine stable.

The dynamics of a cold-to-warm heat engine set up a delicate balance, consistent with the earlier of the Pacific Ocean see-saw (Walker and Bliss, 1932). The atmosphere above maintains a counterbalance, with patch and pacemaker experiments with imposed changes in SST showing the eastern Pacific as a region with high cloud feedback on warming of SST and the warm pool a region of low or even negative feedback (Zhou et al., 2017;Andrews and Webb, 2018).

During the historical period, the heat engine has occupied two states: a relaxed (free) state to the 1950s–1960s dominated by internal variability and a tightly coupled (forced) state thereafter dominated by external forcing. Under forcing the pressure on the heat engine to maintain its constant 'uphill' gradient will come from the supply of additional heat energy and demand for meridional dissipation. Shifts in TEP are roughly twice as large as those in TWP (0.46 °C vs 0.24 °C) and half as frequent.

The maintenance of a constant temperature between TWP and TEP over time while the climate system has evolved from free to forced mode evokes homeostasis. The cold reservoir is the more stable, and although the Pacific cold tongue extends into the eastern Pacific, its centre of action coincides with the Niño 3.4 area in the central Pacific. The warm pool is the more sensitive part of the engine but is also a net heat sink (Song and Yu, 2013). The heat engine discharges heat convectively from the warm pool and Hadley Cells, and advectively to the Indian Ocean, the Pacific Tropical countercurrent and subtropical gyres. The Pacific tropical countercurrent acts as a counterbalance and is the route travelled during El Niño events.

The warm pool also has a N-S structure that helps maintain symmetry between the hemispheres (Feng et al., 2018;Zhang et al., 2018). Dividing TWP into N-S halves shows subtle differences in shift dates. Both identify 1901, the 1937 shift is correctly identified in the N half compared to 1939 for whole region, while the larger WWII anomaly is biased towards the south, 1995 is prominent in both and 2012 prominent in the N (Note this is more recent version of the original data and was averaged differently, so annual results differ slightly, although the monthly shift dates remain the same).

When climate is close to external equilibrium, the heat engine is in free mode and dominated by TEP and shifts can be positive or negative depending on the direction of forcing. GMST is free to follow random walks influenced by the AMO. The heat engine itself is loosely coupled and exchanges heat with the tropical oceans. ENSO has its strongest influence on tropical regions and weaker elsewhere. In this mode, regime shifts can originate in the extratropics and the heat engine will warm or cool in response. It this occurs in one hemisphere, such adjustments may maintain the symmetry in dissipation rates between the hemispheres – in GCMs the transfer of energy to rebalance asymmetric warming occurs quickly (Haywood et al., 2016;Hawcroft et al., 2018).

Forced mode denotes an imbalance between the supply of heat and the capacity of the climate to dissipate it, which can be under or oversupply. The build-up of heat causes SST to whiten initially, followed by land temperatures. The heat engine

https://doi.org/10.5194/esd-2021-61
Preprint. Discussion started: 22 July 2021

becomes tightly coupled and the oscillating mechanism between TWP and TEP, acting like a nonperiodic pendulum, intensifies. The heat engine is the major node within a teleconnected climate network. This allows two-way coupling with higher latitudes, and with other ocean basins, principally with the AMO and AMOC. Governing principles for how the heat engine and its network self-regulate are explored in Paper 2.

4 Conclusions

Severe testing carried out in JR17 confirmed that the staircase identified in historical warming (Jones, 2012;Reid and Beaugrand, 2012;Jones et al., 2013;Belolipetsky et al., 2015) is a response to external forcing dominated by greenhouse gases. This began a search to identify the mechanisms involved, which focused on a sea-level tipping mechanism (Peyser et al., 2016;Yin et al., 2018) involved in the last two global regime shifts. Subsequent analysis revealed the Pacific Ocean heat engine, presented in this paper. The heat engine is technically a heat pump, where the central-eastern Pacific forms the cool reservoir and the western Pacific Warm Pool forms the warm reservoir. This is linked to the broader climate network via circulation and teleconnection.

An early hypothesis was that the warm pool as represented by TWP acts as a thermostat. Based on the analyses presented here and the identification of natural heat pump structure that can tip both warmer and cooler depending on energy supply, we now consider the whole structure outlined in Fig. 19 acts as a thermostat, maintaining climate in a stable state. It can initiate changes, as was the case in 1976–77 and 2013–14, respond to external triggers as in the signal from the AMO in 1995, and adjust to extratropical regime shifts, as was the case in 1901–02 and 1920.

After carrying out a variety of analyses including the detailed tracking of regime shifts, tests on correlation, autocorrelation and Granger analysis, our main conclusions are:

- A heat engine in the tropical Pacific consisting of the eastern-central Pacific (TEP) and western Pacific warm pool (TWP) forms a network with climatic oscillations including the Pacific Decadal Oscillation (PDO) and Atlantic Multidecadal Oscillation (AMO).
- The cold-to-warm structure of the heat engine describes a heat pump sustained by kinetic energy capable of shifting warmer or cooler depending on the direction of forcing.
- The heat engine and broader climate network maintains steady-state regimes with the shallow ocean absorbing all the additional heat from radiative forcing not taken up by irreversible processes.
- Heat stored in the ocean is released as part of a regime shift when an energy imbalance destabilises the existing dissipation process. Regime shifts occur in response to a combination of internal and external forcing.
- Historically, climate has occupied two modes:
    - a free mode from the pre-industrial era to the late 1950s and 1960s, characterised by circulation-dominated dissipation and a relatively weak ENSO. After a cooling episode in the early 1900s the ocean absorbed

https://doi.org/10.5194/esd-2021-61
Preprint. Discussion started: 22 July 2021


Earth System Dynamics Discussions

excess heat through to the late 1930s, most regime shifts appear to be generated from the NH extratropics, warming the tropics and SH.

- a forced mode from the late 1960s. Dissipation rates accelerate and the heat engine works harder, generating white noise in climate data, the climate network becomes more teleconnected switching from slow to fast modes, regime shifts are generated in the tropics, most mediated by the heat engine and propagated poleward.

- During regime shifts in forced mode, mean sea surface temperatures shift upward in the tropics, followed by the extratropics and land with El Niño being the major distributor of heat.
- Rather than a complicated arrangement of signal and noise, climate change is a complex system process best understood as enhanced climate variability.

Paper 2 focuses on the behaviour of climate as a complex system. It proposes a missing step in current conceptual model for how climate changes by identifying a role for thermodynamic forcing. It investigates how the heat engine is represented in the CMIP5 ensemble of coupled climate models. The importance of boundary conditions on complex system behaviour, especially meridional heat transport is explored. The issue of emergence and underdetermination of complex systems within models is also raised as an explanation as to why there are so many alternative theories for phenomena such as ENSO. Finally, it argues that climate is a self-regulating complex system rather than a deterministic stochastic system as it is currently understood.

5 Code availability

The experimental version of the MSBV code used here can be found in Jones and Ricketts (2021a), in addition to a manual version in Microsoft Excel©. As this material is still in review, reviewer access is via: https://datadryad.org/stash/share/7OmkMfNbdgFdPIxvD5qyqhmrzh69ug_tT5MNZ2JMPTQ

6 Data availability

The data generated, tracking model and data for the figures can also be found in Jones and Ricketts (2021a) at https://doi.org/10.5061/dryad.n02v6wwsp. As this material is still in review, reviewer access is via: https://datadryad.org/stash/share/7OmkMfNbdgFdPIxvD5qyqhmrzh69ug_tT5MNZ2JMPTQ

7 Author contributions

RJ conceived the study, JR coded and tested the multi-step model and developed the post-step verification detailed in the SI, both conducted analyses, RJ led the paper with contributions from JR.

https://doi.org/10.5194/esd-2021-61
Preprint. Discussion started: 22 July 2021


Earth System Dynamics Discussions Open Access EGU

8 Competing interests

The authors declare that they have no conflict of interests.

9 Acknowledgements

We would like to thank Pavel Belolipetsky and two anonymous reviewers whose efforts have led us to make substantial improvements to the paper. Data sources include the National Oceanographic Data Center and United States National Climatic Data Center, UK Met Office Hadley Centre, the KNMI climate explorer, and the IRI/LDEO Climate Data Library Colombia University.

10 References

Alheit, J., Licandro, P., Coombs, S., Garcia, A., Giráldez, A., Santamaría, M. T. G., Slotte, A., and Tsikliras, A. C.: Atlantic Multidecadal Oscillation (AMO) modulates dynamics of small pelagic fishes and ecosystem regime shifts in the eastern North and Central Atlantic, J Mar Syst, 133, 88-102, 2014.

Alheit, J., Gröger, J., Licandro, P., McQuinn, I. H., Pohlmann, T., and Tsikliras, A. C.: What happened in the mid-1990s? The coupled ocean-atmosphere processes behind climate-induced ecosystem changes in the Northeast Atlantic and the Mediterranean, Deep Sea Res Part II, 159, 130-142, https://doi.org/10.1016/j.dsr2.2018.11.011, 2019.

Allen, R. J., and Amaya, D. J.: The importance of ENSO/PDO to recent tropical widening, US CLIVAR Variations, 16, 8, 2018.

Anderson, P. W.: More Is Different, Science, 177, 393-396, 10.1126/science.177.4047.393, 1972.

Andrews, T., and Webb, M. J.: The dependence of global cloud and lapse rate feedbacks on the spatial structure of tropical Pacific warming, J Clim, 31, 641-654, https://doi.org/10.1175/jcli-d-17-0087.1, 2018.

Auyang, S. Y.: Foundations of complex-system theories: in economics, evolutionary biology, and statistical physics, Cambridge University Press, 1998.

Bartsev, S., Belolipetskii, P., and Degermendzhi, A.: Multistable states in the biosphere-climate system: towards conceptual models, IOP Conf Ser: Mater Sci Eng, 173, 012005, 2017.

Bartsev, S. I., Belolipetskii, P. V., Degermendzhi, A. G., Ivanova, Y. D., Pochekutov, A. A., and Saltykov, M. Y.: Refocusing on the dynamics of the Earth's climate, Her Russ Acad Sci, 86, 135-142, http://dx.doi.org/10.1134/s1019331616020015, 2016.

Beaugrand, G.: The North Sea regime shift: evidence, causes, mechanisms and consequences, Prog Oceanogr, 60, 245-262, 2004.

https://doi.org/10.5194/esd-2021-61
Preprint. Discussion started: 22 July 2021

Beaugrand, G., Conversi, A., Atkinson, A., Cloern, J., Chiba, S., Fonda-Umani, S., Kirby, R. R., Greene, C. H., Goberville, E., Otto, S. A., Reid, P. C., Stemmann, L., and Edwards, M.: Prediction of unprecedented biological shifts in the global ocean, Nat Clim Change, 9, 237-243, http://dx.doi.org/10.1038/s41558-019-0420-1, 2019.

Beaulieu, C., and Killick, R.: Distinguishing trends and shifts from memory in climate data, J Clim, 2018.

Bejan, A.: Thermodynamics of heating, Proceedings of the Royal Society A, 475, 20180820, 2019.

Belolipetsky, P. V.: The Shifts Hypothesis - an alternative view of global climate change, arXiv preprint arXiv:1406.5805, arXiv:1406.5805, 2014.

Belolipetsky, P. V., Bartsev, S., Ivanova, Y., and Saltykov, M.: Hidden staircase signal in recent climate dynamic, Asia-Pac J Atmos Sci, 51, 323-330, 10.1007/s13143-015-0081-6, 2015.

Bigg, G.: El Nino and the southern oscillation, Weather, 45, 2-8, 1990.

Bindoff, N. L., Stott, P. A., AchutaRao, K. M., Allen, M., Gillett, N., Gutzler, D., Hansingo, K., Hegerl, G., Hu, Y., Jain, S., Mokhov, I., Overland, J., Perlwitz, J., Sebbari, R., and Zhang, X.: Detection and Attribution of Climate Change: from Global to Regional, in: Climate Change 2013: The Physical Science Basis. Working Group I contribution to the IPCC 5th Assessment Report, edited by: Stocker, T. F., Qin, D., Plattner, G.-K., Tignor, M., Allen, S. K., Boschung, J., Nauels, A., Xia, Y., Bex, V., and Midgley, P. M., Cambridge University Press, Cambridge and New York, 132, 2013.

Birkel, S. D., Mayewski, P. A., Maasch, K. A., Kurbatov, A. V., and Lyon, B.: Evidence for a volcanic underpinning of the Atlantic multidecadal oscillation, npj Clim Atmos Sci, 1, 24, http://dx.doi.org/10.1038/s41612-018-0036-6, 2018.

Bjerknes, J.: Atmospheric teleconnections from the equatorial Pacific, Mon Weather Rev, 97, 163-172, 1969.

Bonfils, C., and Santer, B. D.: Investigating the possibility of a human component in various Pacific decadal oscillation indices, Clim Dyn, 37, 1457-1468, 2011.

Bosc, C., Delcroix, T., and Maes, C.: Barrier layer variability in the western Pacific warm pool from 2000 to 2007, Journal of Geophysical Research: Oceans, 114, C06023, 10.1029/2008JC005187, 2009.

Broecker, W. S.: Global warming: Take action or wait?, Jokull, 1-16, 2005.

Bryan, K.: Measurements of meridional heat transport by ocean currents, J Geophys Res, 67, 3403-3414, 1962.

Caesar, L., Rahmstorf, S., Robinson, A., Feulner, G., and Saba, V.: Observed fingerprint of a weakening Atlantic Ocean overturning circulation, Nature, 556, 191, 2018.

Cane, M., and Clement, A. C.: A role for the tropical Pacific coupled ocean-atmosphere system on Milankovitch and millennial timescales. Part II: Global impacts, Mechanisms of global climate change at millennial time scales, 112, 373-383, 1999.

Cane, M. A.: A Role for the Tropical Pacific, Science, 282, 59-61, http://dx.doi.org/10.1126/science.282.5386.59, 1998.

Cassou, C., Kushnir, Y., Hawkins, E., Pirani, A., Kucharski, F., Kang, I.-S., and Caltabiano, N.: Decadal Climate Variability and Predictability: Challenges and Opportunities, Bull Am Meteorol Soc, 99, 479-490, 10.1175/bams-d-16-0286.1, 2018.

Chen, X., and Wallace, J. M.: ENSO-like variability: 1900–2013, J Clim, 28, 9623-9641, 2015.

https://doi.org/10.5194/esd-2021-61
Preprint. Discussion started: 22 July 2021

Chikamoto, Y., Kimoto, M., Ishii, M., Watanabe, M., Nozawa, T., Mochizuki, T., Tatebe, H., Sakamoto, T. T., Komuro, Y., and Shiogama, H.: Predictability of a stepwise shift in Pacific climate during the late 1990s in hindcast experiments using MIROC, J Meteorolog Soc Jpn, 90, 1-21, 2012.

Clement, A. C., and Cane, M.: A role for the tropical Pacific coupled ocean-atmosphere system on Milankovitch and millennial timescales. Part I: A modeling study of tropical Pacific variability, in: Mechanisms of Global Climate Change at Millennial Time Scales, 1999, Blackwell Publishing Ltd, 1999.

Conversi, A., Fonda Umani, S., Peluso, T., Molinero, J. C., Santojanni, A., and Edwards, M.: The Mediterranean Sea regime shift at the end of the 1980s, and intriguing parallelisms with other European basins, PLoS One, 5, e10633, 2010.

Cravatte, S., Delcroix, T., Zhang, D., McPhaden, M., and Leloup, J.: Observed freshening and warming of the western Pacific Warm Pool, Clim Dyn, 33, 565-589, https://doi.org/10.1007/s00382-009-0526-7, 2009.

d'Orgeville, M., and Peltier, W. R.: On the Pacific decadal oscillation and the Atlantic multidecadal oscillation: Might they be related?, Geophys Res Lett, 34, 2007.

De Deckker, P.: The Indo-Pacific Warm Pool: critical to world oceanography and world climate, Geosci Lett, 3, 20, 2016.

Delgado-Bonal, A.: Entropy of radiation: the unseen side of light, Sci Rep, 7, 1642, https://doi.org/10.1038/s41598-017-01622-6, 2017.

Dijkstra, H. A., and Neelin, J. D.: Ocean-atmosphere interaction and the tropical climatology. Part II: Why the Pacific cold tongue is in the east, J Clim, 8, 1343-1359, 1995.

Dijkstra, H. A.: Numerical bifurcation methods applied to climate models: analysis beyond simulation, Nonlin. Processes Geophys., 26, 359-369, 10.5194/npg-26-359-2019, 2019.

Dima, M., and Lohmann, G.: Evidence for Two Distinct Modes of Large-Scale Ocean Circulation Changes over the Last Century, J Clim, 23, 5-16, https://doi.org/10.1175/2009jcli2867.1, 2010.

Dong, B., Sutton, R. T., and Scaife, A. A.: Multidecadal modulation of El Niño–Southern Oscillation (ENSO) variance by Atlantic Ocean sea surface temperatures, Geophys Res Lett, 33, 2006.

Dong, L., Zhou, T., and Chen, X.: Changes of Pacific decadal variability in the twentieth century driven by internal variability, greenhouse gases, and aerosols, Geophys Res Lett, 41, 8570-8577, 2014.

Donges, J. F., Zou, Y., Marwan, N., and Kurths, J.: Complex networks in climate dynamics, The European Physical Journal Special Topics, 174, 157-179, 2009.

Egorova, T., Rozanov, E., Arsenovic, P., Peter, T., and Schmutz, W.: Contributions of natural and anthropogenic forcing agents to the early 20th century warming, Front Earth Sci, 6, 206, 2018.

Enfield, D. B., Mestas-Nuñez, A. M., and Trimble, P. J.: The Atlantic multidecadal oscillation and its relation to rainfall and river flows in the continental US, Geophys Res Lett, 28, 2077-2080, 2001.

Enfield, D. B., and Cid-Serrano, L.: Projecting the risk of future climate shifts, Int J Climatol, 26, 885-895, 2006.

Faranda, D., Messori, G., and Vannitsem, S.: Attractor dimension of time-averaged climate observables: insights from a low-order ocean-atmosphere model, Tellus A: Dynamic Meteorology and Oceanography, 71, 1554413, 2019.

https://doi.org/10.5194/esd-2021-61
Preprint. Discussion started: 22 July 2021

955 Feidt, M.: Thermodynamics applied to reverse cycle machines, a review, Int J Refrig, 33, 1327-1342, 2010.
Feng, J., Li, J., Kucharski, F., Wang, Y., Sun, C., Xie, F., and Yang, Y.: Modulation of the Meridional Structures of the Indo-Pacific Warm Pool on the Response of the Hadley Circulation to Tropical SST, J Clim, 31, 8971-8984, 10.1175/jcli-d-18-0305.1, 2018.
Folland, C. K., Boucher, O., Colman, A., and Parker, D. E.: Causes of irregularities in trends of global mean surface
960 temperature since the late 19th century, Sci Adv, 4, eaao5297, https://doi.org/10.1126/sciadv.aao5297, 2018.
Franzke, C.: Nonlinear trends, long-range dependence, and climate noise properties of surface temperature, J Clim, 25, 4172-4183, 2012.
Fu, R., Del Genio, A. D., and Rossow, W. B.: Influence of Ocean Surface Conditions on Atmospheric Vertical Thermodynamic Structure and Deep Convection, J Clim, 7, 1092-1108, 10.1175/1520-
965 0442(1994)007<1092:ioosco>2.0.co;2, 1994.
Gagan, M. K., Hendy, E. J., Haberle, S. G., and Hantoro, W. S.: Post-glacial evolution of the Indo-Pacific warm pool and El Nino-Southern Oscillation, Quat Int, 118, 127-143, 2004.
Gill, A. E.: Some simple solutions for heat-induced tropical circulation, Q J R Meteorolog Soc, 106, 447-462, 1980.
Gray, S. T., Betancourt, J. L., Fastie, C. L., and Jackson, S. T.: Patterns and sources of multidecadal oscillations in drought-
970 sensitive tree-ring records from the central and southern Rocky Mountains, Geophys Res Lett, 30, 2003.
Hare, S. R., and Mantua, N. J.: An historical narrative on the Pacific Decadal Oscillation, interdecadal climate variability and ecosystem impacts, 20th NE Pacific Pink and Chum workshop, Seattle, WA, 22 March 2001, 2001.
Harries, W., Llewellyn Jones, D., Minnett, P. J., Saunders, R., and Zavody, A.: Observations of sea-surface temperature for climate research, Philos T R Soc S-A, 309, 381-395, 1983.
975 Hawcroft, M., Haywood, J. M., Collins, M., and Jones, A.: The contrasting climate response to tropical and extratropical energy perturbations, Clim Dyn, 1-19, 2018.
Haywood, J. M., Jones, A., Dunstone, N., Milton, S., Vellinga, M., Bodas-Salcedo, A., Hawcroft, M., Kravitz, B., Cole, J., and Watanabe, S.: The impact of equilibrating hemispheric albedos on tropical performance in the HadGEM2-ES coupled climate model, Geophys Res Lett, 43, 395-403, 2016.
980 Hegerl, G. C., Brönnimann, S., Schurer, A., and Cowan, T.: The early 20th century warming: Anomalies, causes, and consequences, Wiley Interdiscip Rev Clim Change, 9, e522, 2018.
Henley, B. J., Gergis, J., Karoly, D. J., Power, S., Kennedy, J., and Folland, C. K.: A tripole index for the interdecadal Pacific oscillation, Clim Dyn, 45, 3077-3090, 2015.
Hidouri, K., and Mohanraj, M.: Thermodynamic analysis of a heat pump assisted active solar still, Desalin Water Treat, 154,
985 101-110, 2019.
Hsu, H. H., and Chen, Y. L.: Decadal to bi-decadal rainfall variation in the western Pacific: A footprint of South Pacific decadal variability?, Geophys Res Lett, 38, 2011.

https://doi.org/10.5194/esd-2021-61
Preprint. Discussion started: 22 July 2021

Hu, D., Wang, F., Sprintall, J., Wu, L., Riser, S., Cravatte, S., Gordon, A., Zhang, L., Chen, D., and Zhou, H.: Review on observational studies of western tropical Pacific Ocean circulation and climate, Journal of Oceanology and Limnology, 38, 906-929, 2020.

Huang, B., Thorne, P. W., Banzon, V. F., Boyer, T., Chepurin, G., Lawrimore, J. H., Menne, M. J., Smith, T. M., Vose, R. S., and Zhang, H.-M.: Extended reconstructed sea surface temperature, version 5 (ERSSTv5): upgrades, validations, and intercomparisons, J Clim, 30, 8179-8205, 2017.

IPCC: Climate Change 2013: The Physical Science Basis. Contribution of Working Group I to the Fifth Assessment Report of the Intergovernmental Panel on Climate Change edited by: Stocker, T. F., Qin, D., Plattner, G.-K., Tignor, M., Allen, S. K., Boschung, J., Nauels, A., Xia, Y., Bex, V., and Midgley, P. M., Cambridge University Press, Cambridge, United Kingdom and New York, NY, USA, 1535 pp., 2013.

Ishii, M., and Kimoto, M.: Reevaluation of historical ocean heat content variations with time-varying XBT and MBT depth bias corrections, J Oceanogr, 65, 287-299, 2009.

Ji, F., Wu, Z., Huang, J., and Chassignet, E. P.: Evolution of land surface air temperature trend, Nat Clim Change, 4, 462-466, 10.1038/nclimate2223, 2014.

Johnson, H. L., Cessi, P., Marshall, D. P., Schloesser, F., and Spall, M. A.: Recent Contributions of Theory to Our Understanding of the Atlantic Meridional Overturning Circulation, Journal of Geophysical Research: Oceans, 124, 5376-5399, 10.1029/2019jc015330, 2019.

Johnson, N. C., Amaya, D. J., Ding, Q., Kosaka, Y., Tokinaga, H., and Xie, S.-P.: Multidecadal modulations of key metrics of global climate change, Global Planet Change, 188, 103149, https://doi.org/10.1016/j.gloplacha.2020.103149, 2020a.

Johnson, Z. F., Chikamoto, Y., Wang, S.-Y. S., McPhaden, M. J., and Mochizuki, T.: Pacific decadal oscillation remotely forced by the equatorial Pacific and the Atlantic Oceans, Clim Dyn, 55, 789-811, 2020b.

Jones, R. N.: Detecting and attributing nonlinear anthropogenic regional warming in southeastern Australia, J Geophys Res, 117, D04105, https://doi.org/10.1029/2011jd016328, 2012.

Jones, R. N., Young, C. K., Handmer, J., Keating, A., Mekala, G. D., and Sheehan, P.: Valuing Adaptation under Rapid Change, National Climate Change Adaptation Research Facility, Gold Coast, Australia, 182 pp., 2013.

Jones, R. N., and Ricketts, J. H.: Reconciling the signal and noise of atmospheric warming on decadal timescales, Earth Syst Dyn, 8, 177-210, 10.5194/esd-8-177-2017, 2017.

Jones, R. N., and Ricketts, J. H.: Shifts to the new abnormal: riding the waves of climate change AJEM Monograph Series, in review, 2019.

Jones, R. N., and Ricketts, J. H.: The Pacific Ocean heat engine: global climate's regulator. Data, Dryad, https://doi.org/10.5061/dryad.n02v6wwsp, 2021a.

Jones, R. N., and Ricketts, J. H.: The Pacific Ocean heat engine, Earth Syst Dyn, submitted, 2021b.

Julian, P. R., and Chervin, R. M.: A study of the Southern Oscillation and Walker Circulation phenomenon, Mon Weather Rev, 106, 1433-1451, 1978.

Kim, B.-M., and An, S.-I.: Understanding ENSO Regime Behavior upon an Increase in the Warm-Pool Temperature Using a Simple ENSO Model, J Clim, 24, 1438-1450, 10.1175/2010jcli3635.1, 2011.

Kim, H. J., An, S. I., and Kim, D.: Timescale-dependent AMOC–AMO relationship in an earth system model of intermediate complexity, Int J Climatol, 41, E3298-E3306, 2021.

Kleidon, A.: Nonequilibrium thermodynamics and maximum entropy production in the Earth system, Naturwissenschaften, 96, 1-25, 2009.

Kleidon, A.: How does the Earth system generate and maintain thermodynamic disequilibrium and what does it imply for the future of the planet?, Philosophical Transactions of the Royal Society A: Mathematical, Physical and Engineering Sciences, 370, 1012-1040, https://doi.org/10.1098/rsta.2011.0316, 2012.

Kleidon, A.: Thermodynamic foundations of the Earth system, Cambridge University Press, 2016.

Knight, J. R., Allan, R. J., Folland, C. K., Vellinga, M., and Mann, M. E.: A signature of persistent natural thermohaline circulation cycles in observed climate, Geophys Res Lett, 32, 2005.

Knight, J. R., Folland, C. K., and Scaife, A. A.: Climate impacts of the Atlantic multidecadal oscillation, Geophys Res Lett, 33, 2006.

Ladyman, J., Lambert, J., and Wiesner, K.: What is a complex system?, European Journal for Philosophy of Science, 3, 33-67, 2013.

Latora, V., and Marchiori, M.: Efficient behavior of small-world networks, Phys Rev Lett, 87, 198701, 2001.

Leith, C. E.: Climate Response and Fluctuation Dissipation, J Atmos Sci, 32, 2022-2026, https://doi.org/10.1175/1520-0469(1975)032<2022:crafd>2.0.co;2, 1975.

Levitus, S., Antonov, J. I., Boyer, T. P., Locarnini, R. A., Garcia, H. E., and Mishonov, A. V.: Global ocean heat content 1955–2008 in light of recently revealed instrumentation problems, Geophys Res Lett, 36, L07608, 10.1029/2008gl037155, 2009.

Li, X., Yang, Y., Li, R., Zhang, L., and Yuan, D.: Structure and dynamics of the Pacific North Equatorial Subsurface Current, Sci Rep, 10, 11758, 10.1038/s41598-020-68605-y, 2020.

Liu, W., Huang, B., Thorne, P. W., Banzon, V. F., Zhang, H.-M., Freeman, E., Lawrimore, J., Peterson, T. C., Smith, T. M., and Woodruff, S. D.: Extended reconstructed sea surface temperature version 4 (ERSST. v4): Part II. Parametric and structural uncertainty estimations, J Clim, 28, 931-951, 2015.

Lorenz, E. N.: Forced and free variations of weather and climate, J Atmos Sci, 36, 1367-1376, 1979.

Lundqvist, P., and Öhman, H.: Global Efficiency of Heat Engines and Heat Pumps with Non-Linear Boundary Conditions, Entropy, 19, 394, 2017.

Ma, J., and Yu, J.-Y.: Linking centennial surface warming patterns in the equatorial Pacific to the relative strengths of the Walker and Hadley circulations, J Atmos Sci, 71, 3454-3464, 2014.

Maes, C., Ando, K., Delcroix, T., Kessler, W. S., McPhaden, M. J., and Roemmich, D.: Observed correlation of surface salinity, temperature and barrier layer at the eastern edge of the western Pacific warm pool, Geophys Res Lett, 33, 2006.

https://doi.org/10.5194/esd-2021-61
Preprint. Discussion started: 22 July 2021

Mantua, N. J., Hare, S. R., Zhang, Y., Wallace, J. M., and Francis, R. C.: A Pacific interdecadal climate oscillation with impacts on salmon production, Bull Am Meteorol Soc, 78, 1069-1079, 1997.

Mantua, N. J., and Hare, S. R.: The Pacific Decadal Oscillation, J Oceanogr, 58, 35-44, 10.1023/a:1015820616384, 2002.

Marini, C., and Frankignoul, C.: An attempt to deconstruct the Atlantic multidecadal oscillation, Clim Dyn, 43, 607-625, 2014.

Mayo, D. G.: Error and the Growth of Experimental Knowledge, University of Chicago Press, Chicago, 509 pp., 1996.

Mayo, D. G.: Evidence as passing severe tests: highly probable versus highly probed hypotheses, in: Scientific Evidence: Philosophical Theories and Applications, edited by: Achinstein, P., John Hopkins University Press, Baltimore and London, 95-127, 2005.

Mayo, D. G.: Learning from error, severe testing, and the growth of theoretical knowledge, in: Error and Inference: Recent Exchanges on Experimental Reasoning, Reliability, and the Objectivity and Rationality of Science, edited by: Mayo, D. G., and Spanos, A., Cambridge University Press, Cambridge UK and New York USA, 28-57, 2010.

Mayo, D. G., and Spanos, A.: Error Statistics, in: Philosophy of Statistics, edited by: Bandyopadhyay, P. S., and Forster, M. R., North-Holland, Amsterdam, 153-198, 2011.

Mayo, D. G.: Statistical Inference as Severe Testing, Cambridge University Press, Cambridge, 486 pp., 2018.

McCabe, G. J., Palecki, M. A., and Betancourt, J. L.: Pacific and Atlantic Ocean influences on multidecadal drought frequency in the United States, Proc Natl Acad Sci USA, 101, 4136-4141, 2004.

Meehl, G. A., Washington, W. M., Wigley, T., Arblaster, J. M., and Dai, A.: Solar and greenhouse gas forcing and climate response in the twentieth century, J Clim, 16, 426-444, 2003.

Neelin, J. D., and Dijkstra, H. A.: Ocean-atmosphere interaction and the tropical climatology. Part I: the dangers of flux correction, J Clim, 8, 1325-1342, 1995.

Newman, M., Compo, G. P., and Alexander, M. A.: ENSO-forced variability of the Pacific decadal oscillation, J Clim, 16, 3853-3857, 2003.

Newman, M., Alexander, M. A., Ault, T. R., Cobb, K. M., Deser, C., Lorenzo, E. D., Mantua, N. J., Miller, A. J., Minobe, S., Nakamura, H., Schneider, N., Vimont, D. J., Phillips, A. S., Scott, J. D., and Smith, C. A.: The Pacific Decadal Oscillation, Revisited, J Clim, 29, 4399-4427, https://doi.org/10.1175/jcli-d-15-0508.1, 2016.

Nicolis, C., and Nicolis, G.: Reconstruction of the dynamics of the climatic system from time-series data, Proceedings of the National Academy of Sciences, 83, 536-540, 10.1073/pnas.83.3.536, 1986.

Nicolis, G.: Physics of far-from-equilibrium systems and self-organisation, in: The New Physics, edited by: Davies, P., Cambridge University Press, Cambridge UK, 316-347, 1992.

Overland, J., Rodionov, S., Minobe, S., and Bond, N.: North Pacific regime shifts: Definitions, issues and recent transitions, Prog Oceanogr, 77, 92-102, 2008.

Ozawa, H., Ohmura, A., Lorenz, R. D., and Pujol, T.: The second law of thermodynamics and the global climate system: A review of the maximum entropy production principle, Rev Geophys, 41, 1018, https://doi.org/10.1029/2002RG000113, 2003.

Park, J.-H., and Li, T.: Interdecadal modulation of El Niño–tropical North Atlantic teleconnection by the Atlantic multi-decadal oscillation, Clim Dyn, 52, 5345-5360, 2019.

Peyser, C. E., Yin, J., Landerer, F. W., and Cole, J. E.: Pacific sea level rise patterns and global surface temperature variability, Geophys Res Lett, 43, 8662–8669, https://doi.org/10.1002/2016GL069401, 2016.

Picaut, J., Ioualalen, M., Menkès, C., Delcroix, T., and Mcphaden, M. J.: Mechanism of the zonal displacements of the Pacific warm pool: Implications for ENSO, Science, 274, 1486-1489, 1996.

Pierrehumbert, R. T.: Climate change and the tropical Pacific: The sleeping dragon wakes, Proc Natl Acad Sci USA, 97, 1355-1358, https://doi.org/10.1073/pnas.97.4.1355, 2000.

Powell Jr, A., and Xu, J.: Decadal regime shift linkage between global marine fish landings and atmospheric planetary wave forcing, Earth Syst Dyn, 6, 2015.

Power, S., Casey, T., Folland, C., Colman, A., and Mehta, V.: Inter-decadal modulation of the impact of ENSO on Australia, Clim Dyn, 15, 319-324, https://doi.org/10.1007/s003820050284, 1999.

Quinn, T. M., Taylor, F. W., and Crowley, T. J.: Coral-based climate variability in the Western Pacific Warm Pool since 1867, Journal of Geophysical Research: Oceans, 111, 2006.

Rahmstorf, S., Box, J. E., Feulner, G., Mann, M. E., Robinson, A., Rutherford, S., and Schaffernicht, E. J.: Exceptional twentieth-century slowdown in Atlantic Ocean overturning circulation, Nat Clim Change, 5, 475, 2015.

Reid, P. C., and Beaugrand, G.: Global synchrony of an accelerating rise in sea surface temperature, J Mar Biol Assoc UK, 92, 1435-1450, https://doi.org/10.1017/S0025315412000549, 2012.

Reid, P. C.: Ocean warming: setting the scene, in: Explaining ocean warming:causes, scale, effects and consequences, edited by: Laffoley, D., and Baxter, J. M., IUCN, Gland, Switzerland, 2016.

Reid, P. C., Hari, R. E., Beaugrand, G., Livingstone, D. M., Marty, C., Straile, D., Barichivich, J., Goberville, E., Adrian, R., and Aono, Y.: Global impacts of the 1980s regime shift, Global Change Biol, 22, 682-703, https://doi.org/10.1111/gcb.13106, 2016.

Ricketts, J., and Jones, R.: Characterizing change-points in climate series with a severe approach, MODSIM2017, 22nd International Congress on Modelling and Simulation, Hobart, Tasmania, 2018.

Ricketts, J. H.: Understanding the Nature of Abrupt Decadal Shifts in a Changing Climate, Ph D (accepted under revision), Institute of Sustainable Industry and Liveable Cities, Victoria University, Melbourne, 2019.

Robson, J., Sutton, R., Lohmann, K., Smith, D., and Palmer, M. D.: Causes of the Rapid Warming of the North Atlantic Ocean in the Mid-1990s, J Clim, 25, 4116-4134, 10.1175/jcli-d-11-00443.1, 2012.

Rodionov, S.: A sequential method of detecting abrupt changes in the correlation coefficient and its application to Bering Sea climate, Climate, 3, 474-491, 2015.

https://doi.org/10.5194/esd-2021-61
Preprint. Discussion started: 22 July 2021

Saltykov, M., Belolipetsky, P., Hari, R., Reid, P., and Bartsev, S.: Synchronous shifts in outgoing longwave radiation and their interpretation, 15th International Conference on Environmental Science and Technology, Rhodes, Greece, 31 August to 2 September 2017, 2017.

Schneider, S. H., and Dickinson, R. E.: Climate modeling, Rev Geophys, 12, 447-493, 1974.

Simpson, J. e.: Report of the science steering group for a tropical rainfall measuring mission (TRMM), National Aeronautics and Space Administration, Greenbelt Maryland, 1988.

Sivakumar, V., and Sundaram, E. G.: Improvement techniques of solar still efficiency: A review, Renewable Sustainable Energy Rev, 28, 246-264, 2013.

Song, X., and Yu, L.: How much net surface heat flux should go into the Western Pacific Warm Pool?, Journal of Geophysical Research: Oceans, 118, 3569-3585, https://doi.org/10.1002/jgrc.20246, 2013.

Stocker, T. F., Qin, D., Plattner, G.-K., Alexander, L. V., Allen, S. K., Bindoff, N. L., Bréon, F.-M., Church, J. A., U. Cubasch, Emori, S., Forster, P., Friedlingstein, P., Gillett, N., Gregory, J. M., Hartmann, D. L., Jansen, E., Kirtman, B., R. Knutti, K., Kumar, K., Lemke, P., Marotzke, J., Masson-Delmotte, V., Meehl, G. A., Mokhov, I. I., Piao, S., Ramaswamy, V., Randall, D., Rhein, M., Rojas, M., Sabine, C., Shindell, D., Talley, L. D., Vaughan, D. G., and Xie, S.-P.: Technical Summary, in: Climate Change 2013: The Physical Science Basis. Contribution of Working Group I to the Fifth Assessment Report of the Intergovernmental Panel on Climate Change, edited by: Stocker, T. F., Qin, D., Plattner, G.-K., M. Tignor, Allen, S. K., Boschung, J., Nauels, A., Xia, Y., Bex, V., and Midgley, P. M., Cambridge University Press, Cambridge, United Kingdom and New York, NY, USA, 33-115, 2013.

Strevens, M.: Bigger than chaos: Understanding complexity through probability, Harvard University Press, 2009.

Sud, Y. C., Walker, G. K., and Lau, K.-M.: Mechanisms regulating sea-surface temperatures and deep convection in the tropics, Geophys Res Lett, 26, 1019-1022, https://doi.org/10.1029/1999GL900197, 1999.

Sun, C., Kucharski, F., Li, J., Jin, F.-F., Kang, I.-S., and Ding, R.: Western tropical Pacific multidecadal variability forced by the Atlantic multidecadal oscillation, Nat Commun, 8, 1-10, 2017.

Sun, C., Zhang, J., Li, X., Shi, C., Gong, Z., Ding, R., Xie, F., and Lou, P.: Atlantic Meridional Overturning Circulation reconstructions and instrumentally observed multidecadal climate variability: A comparison of indicators, Int J Climatol, 41, 763-778, 2021.

Sverdrup, H. U.: Wind-driven currents in a baroclinic ocean; with application to the equatorial currents of the eastern Pacific, Proc Natl Acad Sci USA, 33, 318, 1947.

Swingedouw, D., Mignot, J., Ortega, P., Khodri, M., Menegoz, M., Cassou, C., and Hanquiez, V.: Impact of explosive volcanic eruptions on the main climate variability modes, Global Planet Change, 150, 24-45, 2017.

Tan, K., and Rhodes, B.: Drought severity estimation under a changing climate, Australasian Journal of Water Resources, 17, 143 - 151, 2012.

Thompson, B., Tkalich, P., and Malanotte-Rizzoli, P.: Regime shift of the South China Sea SST in the late 1990s, Clim Dyn, 48, 1873-1882, https://doin.org/10.1007/s00382-016-3178-4, 2017.

https://doi.org/10.5194/esd-2021-61
Preprint. Discussion started: 22 July 2021

Thornalley, D. J. R., Oppo, D. W., Ortega, P., Robson, J. I., Brierley, C. M., Davis, R., Hall, I. R., Moffa-Sanchez, P., Rose, N. L., Spooner, P. T., Yashayaev, I., and Keigwin, L. D.: Anomalously weak Labrador Sea convection and Atlantic overturning during the past 150 years, Nature, 556, 227-230, 10.1038/s41586-018-0007-4, 2018.

Timmermann, A., An, S.-I., Kug, J.-S., Jin, F.-F., Cai, W., Capotondi, A., Cobb, K. M., Lengaigne, M., McPhaden, M. J., Stuecker, M. F., Stein, K., Wittenberg, A. T., Yun, K.-S., Bayr, T., Chen, H.-C., Chikamoto, Y., Dewitte, B., Dommenget, D., Grothe, P., Guilyardi, E., Ham, Y.-G., Hayashi, M., Ineson, S., Kang, D., Kim, S., Kim, W., Lee, J.-Y., Li, T., Luo, J.-J., McGregor, S., Planton, Y., Power, S., Rashid, H., Ren, H.-L., Santoso, A., Takahashi, K., Todd, A., Wang, G., Wang, G., Xie, R., Yang, W.-H., Yeh, S.-W., Yoon, J., Zeller, E., and Zhang, X.: El Niño–Southern Oscillation complexity, Nature, 559, 535-545, 10.1038/s41586-018-0252-6, 2018.

Trenberth, K. E., and Hurrell, J. W.: Decadal atmosphere-ocean variations in the Pacific, Clim Dyn, 9, 303-319, 1994.

Trenberth, K. E., and Shea, D. J.: Atlantic hurricanes and natural variability in 2005, Geophys Res Lett, 33, https://doi.org/10.1029/2006GL026894, 2006.

Tsonis, A. A., and Swanson, K. L.: Climate mode covariability and climate shifts, Int J Bifurcation Chaos, 21, 3549-3556, 2011.

Varotsos, C., Efstathiou, M., and Christodoulakis, J.: Abrupt changes in global tropospheric temperature, Atmos Res, 217, 114-119, 2019.

Walker, G., and Bliss, W.: World weather V, Memoirs of the Royal Meteorological Society 4, 53-84, 1932.

Wang, J., Xu, C., Hu, M., Li, Q., Yan, Z., and Jones, P.: Global land surface air temperature dynamics since 1880, Int J Climatol, 38, e466-e474, 2018.

Watts, D. J., and Strogatz, S. H.: Collective dynamics of 'small-world' networks, Nature, 393, 440-442, 10.1038/30918, 1998.

Weller, E., Min, S.-K., Cai, W., Zwiers, F. W., Kim, Y.-H., and Lee, D.: Human-caused Indo-Pacific warm pool expansion, Sci Adv, 2, e1501719, 2016.

Wheatley, J. C., Swift, G. W., and Migliori, A.: The natural heat engine, Los Alamos Science, 14, 2-33, 1986.

Whetton, P., Adamson, D., and Williams, M.: Rainfall and river flow variability in Africa, Australia and East Asia linked to El Niño-Southern Oscillation events, Geological Society of Australia Symposium Proceedings, 1990, 71-82,

Wolter, K., and Timlin, M. S.: El Niño/Southern Oscillation behaviour since 1871 as diagnosed in an extended multivariate ENSO index (MEI.ext), Int J Climatol, 31, 1074-1087, https://doi.org/10.1002/joc.2336, 2011.

Wu, T., Hu, A., Gao, F., Zhang, J., and Meehl, G. A.: New insights into natural variability and anthropogenic forcing of global/regional climate evolution, npj Clim Atmos Sci, 2, 18, 10.1038/s41612-019-0075-7, 2019.

Wunsch, C.: The total meridional heat flux and its oceanic and atmospheric partition, J Clim, 18, 4374-4380, 2005.

Wunsch, C., and Heimbach, P.: Two decades of the Atlantic meridional overturning circulation: Anatomy, variations, extremes, prediction, and overcoming its limitations, J Clim, 26, 7167-7186, 2013.

Wyrtki, K.: Teleconnections in the equatorial Pacific Ocean, Science, 180, 66-68, 1973.

Wyrtki, K.: El Niño—the dynamic response of the equatorial Pacific Ocean to atmospheric forcing, J Phys Oceanogr, 5, 572-584, 1975a.

Wyrtki, K.: Fluctuations of the dynamic topography in the Pacific Ocean, J Phys Oceanogr, 5, 450-459, 10.1175/1520-0485(1975)005<0450:fotdti>2.0.co;2, 1975b.

Yang, M., Feng, X., and Liu, G.: Heat integration of heat pump assisted distillation into the overall process, Appl Energy, 162, 1-10, https://doi.org/10.1016/j.apenergy.2015.10.044, 2016.

Yin, J., Overpeck, J., Peyser, C., and Stouffer, R.: Big Jump of Record Warm Global Mean Surface Temperature in 2014–2016 Related to Unusually Large Oceanic Heat Releases, Geophys Res Lett, 45, 1069-1078, 2018.

Yu, J.-Y., Kao, P.-k., Paek, H., Hsu, H.-H., Hung, C.-w., Lu, M.-M., and An, S.-I.: Linking emergence of the central Pacific El Niño to the Atlantic multidecadal oscillation, J Clim, 28, 651-662, 2015.

Zhang, L., and Wang, C.: Multidecadal North Atlantic sea surface temperature and Atlantic meridional overturning circulation variability in CMIP5 historical simulations, Journal of Geophysical Research: Oceans, 118, 5772-5791, 2013.

Zhang, R., and Delworth, T. L.: Impact of the Atlantic multidecadal oscillation on North Pacific climate variability, Geophys Res Lett, 34, 2007.

Zhang, R., Sutton, R., Danabasoglu, G., Kwon, Y. O., Marsh, R., Yeager, S. G., Amrhein, D. E., and Little, C. M.: A review of the role of the Atlantic meridional overturning circulation in Atlantic multidecadal variability and associated climate impacts, Rev Geophys, 57, 316-375, 2019.

Zhang, W., Li, J., and Jin, F. F.: Spatial and temporal features of ENSO meridional scales, Geophys Res Lett, 36, L15605, https://doi.org/10.1029/2009GL038672, 2009.

Zhang, Y., Xie, S.-P., Kosaka, Y., and Yang, J.-C.: Pacific Decadal Oscillation: Tropical Pacific Forcing versus Internal Variability, J Clim, 31, 8265-8279, 10.1175/jcli-d-18-0164.1, 2018.

Zhou, C., Zelinka, M. D., and Klein, S. A.: Analyzing the dependence of global cloud feedback on the spatial pattern of sea surface temperature change with a Green's function approach, J Adv Model Earth Syst, 9, 2174-2189, 2017.